NACA RM L50B15

NACA

RESEARCH MEMORANDUM

FULL-SCALE INVESTIGATION OF BOUNDARY-LAYER CONTROL BY SUCTION THROUGH LEADING-EDGE SLOTS ON A WING-FUSELAGE CONFIGURATION HAVING 47.5° LEADING-EDGE SWEEP WITH AND WITHOUT FLAPS

By Jerome Pasamanick and Thomas B. Sellers

Langley Aeronautical Laboratory
Langley Air Force Base, Va.

NATIONAL ADVISORY COMMITTEE
FOR AERONAUTICS
WASHINGTON

April 5, 1950

NACA RM L50B15

NATIONAL ADVISORY COMMITTEE FOR AERONAUTICS

RESEARCH MEMORANDUM

FULL-SCALE INVESTIGATION OF BOUNDARY-LAYER CONTROL BY SUCTION THROUGH LEADING-EDGE SLOTS ON A WING-FUSELAGE CONFIGURATION HAVING 47.5° LEADING-EDGE SWEEP WITH AND WITHOUT FLAPS

By Jerome Pasamanick and Thomas B. Sellers

SUMMARY

The effects of suction through slots located at the $\frac{1}{2}$-percent-chord and $2\frac{1}{2}$-percent-chord stations on the longitudinal aerodynamic characteristics of 47.5° sweptback wing-fuselage configuration with and without flaps have been investigated in the Langley full-scale tunnel at an average Reynolds number of 6.1×10^6. The wing section normal to the quarter-chord line was NACA 64_1A112, the aspect ratio was 3.4, and the taper ratio was 0.51.

The maximum-lift coefficient of the plain wing without suction was 1.03 and the application of suction at a high flow rate increased the maximum lift to 1.20. The wing in the sealed and faired condition was longitudinally unstable at stall, but with suction applied along the outboard 73-percent span at the most forward leading-edge slot $\left(\frac{1}{2}\text{-percent chord}\right)$ the instability near maximum lift was eliminated. Applying suction at a high flow rate along the outboard 50-percent wing span with this slot resulted in a maximum-lift coefficient of 1.13 and longitudinal stability throughout the lift range.

The installation of split flaps resulted in maximum-lift values similar to the unflapped wing with and without boundary-layer suction and was longitudinally unstable for all conditions investigated.

The 47-percent-span, 59-percent-span, and 74-percent-span extensible leading-edge flaps combined with suction $\left(2\frac{1}{2}\text{-percent-chord slots}\right)$

at a high flow rate gave maximum-lift increments of 0.06, 0.03, and 0.08, respectively, so that maximum-lift coefficients of 1.19, 1.21, and 1.26 resulted for the respective flap arrangements. The smaller-span leading-edge-flap configurations were longitudinally stable at the stall for the conditions with and without suction; whereas the 74-percent-span-flap configuration was longitudinally stable only at a high-suction-flow rate.

INTRODUCTION

The lift and stability characteristics of thin sweptback wings are relatively poor as a result of leading-edge separation and thick boundary layers developed over the tip sections. The use of devices such as leading-edge flaps as a means for delaying separation (reference 1) has, in general, shown improvements in the inherently poor low-speed characteristics of thin swept wings. In addition to the use of flaps, the application of suction at the approximate midchord position on a thin two-dimensional airfoil (reference 2) and leading-edge area suction on the same model (reference 3) has also improved the section lift characteristics but, as yet, very few data are available with boundary-layer control on three-dimensional wings. A program was undertaken sometime ago at the Langley full-scale tunnel to evaluate the effects of various combinations of high-lift flaps and the application of boundary-layer control by suction on the longitudinal stability and lift characteristics of a thin highly sweptback wing.

The model investigated had a wing leading-edge sweep of 47.5°, an aspect ratio of 3.4, a taper ratio of 0.51, and NACA 64_1A112 airfoil sections were normal to the quarter-chord line.

The initial phase of the general program was to investigate the effectiveness on the aerodynamic characteristics of suction slots at the 20-percent-chord, 40-percent-chord, and 70-percent-chord stations along the outboard half of the wing span (reference 4). These results indicated that separation occurred at the leading edge and showed the necessity of applying suction near the wing leading edge. The experimental results of reference 5 further indicated that a suction slot located immediately rearward of the peak negative surface pressure would help to eliminate leading-edge separation. The full-scale-tunnel program was, therefore, extended to investigate the control of leading-edge separation by suction and the results of the investigation are presented herein. The slot location required for this control is known to be dependent upon the variations of the pressure distribution or angle of attack and, from the two-dimensional data of reference 5, it is seen

that a suction slot at or very near the $\frac{1}{2}$-percent-chord station was effective in improving the section lift characteristics. The slots for the tests presented herein were therefore located at the $\frac{1}{2}$-percent-chord and the $2\frac{1}{2}$-percent-chord stations and were investigated individually or in combination with the 40-percent-chord suction slots and with split trailing-edge flaps. The $2\frac{1}{2}$-percent-chord slot was also investigated in combination with the extensible leading-edge flaps. The average Reynolds number for the tests with suction was 6.1×10^6 and the Mach number was approximately 0.10.

SYMBOLS

C_L lift coefficient $\left(\frac{L}{q_o S}\right)$

c_l section lift coefficient $\left(\cos \alpha \int_0^{c'} P \frac{dx}{c'}\right)$

C_D drag coefficient $\left(\frac{D}{q_o S}\right)$

C_m pitching-moment coefficient $\left(\frac{M}{q_o S \bar{c}}\right)$

C_Q suction-flow coefficient $\left(\frac{Q}{V_o S'}\right)$

C_p pressure-loss coefficient $\left(\frac{H_o - H_d}{q_o}\right)$

P pressure coefficient $\left(\frac{p - p_o}{q_o}\right)$

L lift, pounds

l	section lift, pounds
D	drag, pounds
M	pitching moment; positive when moment tends to increase angle of attack, foot-pounds
S	total wing area, square feet
S'	wing area affected by span of suction slots, square feet
q_o	free-stream dynamic pressure, pounds per square foot $\left(\frac{1}{2}\rho_o V_o^2\right)$
ρ_o	mass density of air, slugs per cubic foot
V_o	free-stream velocity, feet per second
c	wing chord measured perpendicular to quarter-chord line, feet
c'	wing chord measured parallel to plane of symmetry, feet
$\bar{c}$	wing mean aerodynamic chord measured in plane parallel to plane of symmetry, feet $\left(\frac{2}{S}\int_0^{b/2} c'^2 dy\right)$
Q	total quantity flow through suction slots, cubic feet per second
H_o	free-stream total pressure, pounds per square foot
H_d	total pressure inside wing duct, pounds per square foot
p	local static pressure, pounds per square foot
p_o	free-stream static pressure, pounds per square foot
R	Reynolds number $\left(\frac{\rho_o V_o \bar{c}}{\mu}\right)$
μ	coefficient of viscosity, slugs per foot-second

x	distance measured parallel to plane of symmetry, feet
y	distance measured perpendicular to plane of symmetry, feet
b	wing span measured perpendicular to plane of symmetry, feet
α	angle of attack of wing chord line measured in plane of symmetry, degrees

MODEL

General dimensions of the model are given in the three-view drawing of figure 1, and figure 2 presents a photograph of the model mounted in the Langley full-scale tunnel. The wing leading-edge sweepback was 47.5°, the aspect ratio was 3.4, the taper ratio was 0.51, and the airfoil sections normal to the quarter-chord line were NACA 64_1A112. The wing panels were mounted in a low midwing position at zero incidence on a circular fuselage and had no geometric dihedral and no twist.

The auxiliary high-lift devices tested in conjunction with boundary-layer control consisted of extensible leading-edge flaps and split trailing-edge flaps. Details of the flaps are given in figure 3. The extensible leading-edge flaps were 10-percent chord and extended over the outboard 47, 59, and 74 percent of each wing panel and were deflected 127.5° from the wing chord line. These leading-edge flaps were faired into the wing surface and, for these particular configurations, it was not possible to test the flaps in conjunction with the $\frac{1}{2}$-percent-chord slots. The 20-percent-chord split flaps extended outboard from the 12-percent-semispan station to the 56-percent-semispan station and were deflected 60° from the wing chord line (measured in a plane parallel to the plane of symmetry).

Boundary-layer suction was applied at the wing upper surface through slots located at either the 0.005c or 0.025c, and in combination with slots at the 0.40c stations (fig. 3). The leading-edge slots spanned the outboard 73 percent of each wing panel and the 40-percent-chord slots extended outboard from the 51-percent-semispan station to the 94-percent-semispan station. The area affected by the 73-percent-span leading-edge suction slots was 67.4 percent of the total wing area. Sealing the inboard 23-percent span of these slots reduced the affected wing area to 40.7 percent of the total wing area. The slots discharged the air into a single box-beam type of passage that was used as a duct to the axial-flow blower housed in the fuselage (fig. 4 of reference 4).

Flow quantities were determined from a large number of total- and static-pressure measurements in the annulus ahead of the axial-flow blower. It would have been desirable to have obtained pressure measurements in the slot diffuser along the span, but such instrumentation was not installed in the model and, therefore, the pressure-loss coefficients C_p were determined from total-pressure measurements obtained at the wing-fuselage juncture of each wing panel, where the total pressure was essentially static pressure because of the low velocity. From the results of the investigation reported in reference 4 it was evident that pressure-distribution data over a few spanwise stations would be most useful in the interpretation of the wing-stall progression and in the evaluation of the local influences of boundary-layer suction. Airfoil surface pressures (measured in a plane parallel to the plane of symmetry, table I) were measured over the left wing panel by flush orifices located at the $0.34\frac{b}{2}$, $0.53\frac{b}{2}$, $0.73\frac{b}{2}$, and $0.93\frac{b}{2}$ stations.

TESTS AND METHODS

The tests to determine the effects of leading-edge suction on the longitudinal aerodynamic characteristics of the model were made on the six-component-balance system of the Langley full-scale tunnel. Force data, airfoil pressure distributions, and upper-surface tuft observations were obtained at zero yaw over a range of angle of attack from small negative angles to the angle for maximum lift (except for two conditions where the maximum lift was not clearly defined).

Boundary-layer suction data were obtained with slots located at the 0.005c and 0.025c stations, and these slots were investigated separately and in combination with the 0.40c slot installation. A few tests were made to determine the effects of reducing the spanwise extent of the 0.005c leading-edge slots by sealing the inboard 23-percent span of these slots. The effects of sudden loss of boundary-layer suction simulating a power failure by having the slots open and allowing the blower to windmill were investigated for the plain-wing configuration having the $0.73\frac{b}{2}$ 0.005c slots. Because the $0.74\frac{b}{2}$ extensible leading-edge-flap installation was found to produce the highest $C_{L_{max}}$ and longitudinal stability at stall when combined with suction at the 0.025c slots, a similar power-failure test was conducted.

A few exploratory tests were made to determine if there were any appreciable low-speed scale effects for the plain wing and the wing with split flaps without boundary-layer control from 2.2 to 7.5×10^6

and from 2.2 to 6.1 × 10^6, respectively. The tests to investigate boundary-layer suction were made at a Reynolds number of 6.1 × 10^6 and a Mach number of about 0.10.

The operational characteristics of the large (3-foot-diameter), single-stage, axial-flow blower used in this investigation were such that, to obtain the required pressure rise, relatively large air quantities were drawn through the system. The attempts to control the quantity at any condition by throttling or auxiliary bleed were not successful because of the accompanied reductions in pressure rise, and, in some instances, even for an unthrottled condition, the fan was receiving insufficient air-flow quantity for maximum pressure rise. In all cases, the flow rates that were encountered are greater than those recorded in two-dimensional investigations (references 3 and 5). The tests were run at constant speeds of either 3000 or 4000 rpm producing total-suction-flow coefficients of the order of 0.01 to about 0.035 and pressure-loss coefficients from about 4 to 10 over the complete range of angle of attack, and these data are presented with the force data. The zero-flow-rate condition represents the configuration with the slots sealed and faired to a smooth contour with the wing.

RESULTS

The data have been corrected for jet-boundary effects (as determined from the straight-wing method of reference 6), blocking effects, stream alinement, and approximate wing-support interference. In addition, a drag tare correction has been applied to compensate for the effects of the air-jet thrust due to the blower operation. The drag coefficients, as presented in the figures, are the measured coefficients of the external drag of the wing-fuselage combination and do not include the blower-power drag coefficients. In determining the section lift characteristics, a check of the chordwise-force component in the high angle-of-attack range showed that it could contribute only 3 percent to the lift and this component was therefore neglected.

In any comparison of these results with those of the investigation presented in reference 4 it should be noted that the aspect ratio of the model was reduced from 3.5 to 3.42, the taper ratio was changed from 0.50 to 0.51, and the location of the quarter chord of the mean aerodynamic chord was shifted slightly forward. These plan-form variations did not appreciably affect the lift and drag characteristics but did affect somewhat the longitudinal stability characteristics of the model.

The surface-pressure results presented were obtained at only four spanwise stations; hence they are not sufficiently extensive for a

loads analysis but do provide some detailed information regarding the flow phenomena for the conditions investigated. In all cases with the semispan split flaps deflected, section lift coefficients are not presented for the two inboard stations because of the absence of pressure measurements over the rearward part of the wing and flaps; however, the airfoil surface pressures are presented to show the important effects in the region of the wing leading edge.

A summary of the maximum-lift results and the longitudinal stability characteristics for the wing configurations tested are presented in table II. In order to facilitate the discussion of the results, the data are arranged in the following order of figures. The results of the Reynolds number tests for the plain wing and the wing with split flaps are presented in figure 4. Figures 5 and 6 present force-test data and visual tuft diagrams for the plain-wing configuration with and without boundary-layer suction and various slot locations. The split-flap tests with suction at the 0.005c slot and the combination of the 0.005c slot and the 0.40c slot are shown in figure 7, and the associated stall diagrams are given in figure 8. Force-test data and flow diagrams for the condition with suction at the 0.025c slots, and the combination of the 0.025c slot and the 0.40c slot, and with extensible leading-edge flaps are given in figures 9 and 10. Airfoil-surface-pressure data for the plain wing and the wing with split flaps are presented in figures 11 and 12 for the conditions with and without boundary-layer suction. Summary curves of section lift data as obtained by integrating the chordwise-surface pressures for several Reynolds numbers are given in figure 13 for the plain wing and for the wing with split flaps. Figure 14 presents section lift data for the plain wing and the wing with split flaps showing the effects of leading-edge suction. The effects of the extensible leading-edge flaps without boundary-layer control on the chordwise-pressure distributions are given in figure 15. The effects of suction-power failure on the characteristics of the model for the plain wing and the wing with $0.74\frac{b}{2}$ extensible leading-edge flaps are given in figure 16.

DISCUSSION

Reynolds Number Effect

In order to determine if there were any scale effects in the low-speed range on the characteristics of the present wing, preliminary tests were made for the plain wing and the wing with split flaps and slots in the sealed and faired condition. The results indicate that varying the Reynolds number had no appreciable effects on the lift and

drag characteristics of the model in the low- and moderate-lift-coefficient range. The greatest increase in the maximum-lift coefficients occurred between Reynolds numbers of 3.0×10^6 and 5.2×10^6, and the results of figure 4 show increments of about 0.04 and 0.09 for the plain wing and the wing with split flaps, respectively. The section lift plots of figure 13 also show the small influence of Reynolds number, in the range investigated, on the lift characteristics and these results are consistent with the trends shown in figure 4.

The shape of the pitching-moment curves in the low- and moderate-lift-coefficient range was not significantly influenced by increasing the Reynolds number; however, the unstable break in the moment curve occurred at increasingly higher lift coefficients between Reynolds numbers of 3.0×10^6 and 5.2×10^6. For all conditions, the sudden instability in the high-lift range is closely related to the point on the lift curve where initial decrease in lift-curve slope occurs and where the drag-coefficient-curve slope increases rapidly.

Characteristics of the Plain Wing

The maximum-lift coefficient of the plain wing without boundary-layer control was 1.03 at an angle of attack of 21°. In the low-lift-coefficient range, the lift-curve slope as calculated from simple sweep theory (0.057) is in good agreement with the results of figure 5 (0.054) and the pitching-moment characteristics about the quarter chord of the mean aerodynamic chord in this lift-coefficient range show static stability. Between lift coefficients of 0.6 and 0.8, the tuft diagrams (fig. 6) and the airfoil surface pressures (fig. 11) indicate the flow over the tip sections to be disturbed, and a separation bubble was evident at the leading edge of about the $0.93\frac{b}{2}$ station. The presence of this bound region of separation at the leading edge causes an increase in the local-section-lift coefficient as has been shown previously in the investigation of reference 7. This increase in lift over the tip produces the increased stability shown in the lift-coefficient range of about 0.9 (fig. 5). As the angle of attack increases further, the rapid progression of separation over the entire tip produces a very sudden loss of lift over the outboard sections, and, therefore, the severe longitudinal instability prior to $C_{L_{max}}$.

The results with boundary-layer control (fig. 5) show that suction increased the maximum-lift coefficients from 1.03 to 1.12 and to 1.20 at blower speeds of 3000 and 4000 rpm, respectively, for either the 0.005c or the 0.025c slot arrangements. In the angle-of-attack range prior to $C_{L_{max}}$, the lift coefficients with boundary-layer control at

the 0.005c station were slightly lower than those for the sealed wing. The reduction in lift is attributed to the fact that suction prevented the formation of leading-edge separation and thus eliminated the additional increment of lift which had occurred at the tip sections for the basic wing. The linear portions of the lift curve were, however, extended to higher angles of attack and, for the 0.025c slot configurations, suction slightly increased the slope of the lift curve. The application of suction at the 0.005c had no appreciable effects on the pitching-moment characteristics of the wing in the low-lift-coefficient range. In the moderate- and high-lift-coefficient range, however, suction was effective in eliminating the leading-edge separation bubble at the tip and, therefore, prevented the sudden stabilizing tendency previously shown for the plain wing. The flow over the tips was sufficiently controlled to produce more desirable pitching-moment characteristics at maximum lift. The flow diagrams indicate that initial stall occurred over the rear portions of the tip sections and spread inboard along the rear portion of the wing. At angles of attack near $C_{L_{max}}$, intermittent stall occurs at the leading edge, which probably is responsible for the momentary instability indicated for this configuration.

The effectiveness of suction (0.005c slots) on the leading-edge flow is shown by the section lift plots (fig. 14) to be variable over the span and, from such information, it should be possible to ascertain the variations in spanwise control of suction flow which would be required for maximum effectiveness. However, these results show that at the higher angles of attack, which is the most significant range under consideration, with the lower flow rate (3000 rpm) more lift was produced over the inboard sections; whereas a greater flow rate was necessary over the outboard sections to provide any substantial increases in lift. The greater effectiveness of the lower-suction condition over the inboard section would not normally be expected but the following offers a possible explanation for this effect. The average plenum-chamber pressure-loss coefficient C_p (fig. 5(a)) is about 10 and 6 for the 4000- and 3000-rpm suction conditions, respectively. The greater suction condition, in general, produced the required pressure drop to induce inflow along the span of the wing and the lower pressure-loss coefficient (C_p = 6 for 3000 rpm), however, was unable to satisfy the pressure differential required for inflow at the inboard sections. As a result of the spanwise variation in the surface pressures, which can be found from a careful examination of figures 11(c) and 11(d), in particular the pressures at the $2\frac{1}{2}$-percent chordwise station, it is conceivable that air was sucked into the slots along the center and outboard sections and blown out of the slots along the inboard sections. It is possible that the outflow would produce the effect of a local increased camber of the inboard sections (fig. 11(d)), $0.34\frac{b}{2}$ and thus

an increase in lift over the forward portion of the airfoil and some forward shift of the center of pressure. The wing was about neutrally stable up through the stall for the lower suction condition of 3000 rpm, although there was some destabilizing moment shift in the higher lift-coefficient range as compared to the higher suction condition, which is believed to be caused by the forward movement of the center of pressure associated with the outflow over the inboard portions of the slot.

It should be pointed out that in the moderate-lift-coefficient range the section-lift data presented in figure 14 indicate an increase in lift due to suction; whereas the force data presented in figure 5(a) indicate a decrease in lift due to suction. A reason for this discrepancy could not be determined. If it is associated with some measuring inaccuracy, some of the preceding discussion of the possible flow phenomena might lose its significance. It is recognized, in any case, that this discussion is only tentative, although it is felt that the general approach is reasonably correct.

The previous results have shown that suction at the leading edge of the outboard 73 percent of the wing span appreciably improved the longitudinal stability characteristics of the model, but the stall which occurred at high lift coefficients over the outboard sections was not eliminated. The inboard 23 percent of the 0.005c slots were sealed, and the results (fig. 5(a)) indicate that, although the maximum lift was reduced from 1.20, for the wing with 73-percent span 0.005c slots, to 1.13 (at 4000 rpm) the model has more stable pitching-moment characteristics over the lift-coefficient range including a very stable pitching tendency near $C_{L_{max}}$. The greater breakdown in the lift over the inboard sections, for the small-span slot configuration in comparison with that for the large-span slot configuration, resulted in a stabilizing rearward shift of the aerodynamic center and a net decrease in total lift.

Suction-slot location has been shown in the two-dimensional tests of reference 5 to be of primary importance for the control of leading-edge separation on a thin airfoil at high lift coefficients. The present investigation with suction at the 0.025c slots also clearly indicates the significance of slot location. The pitching-moment curves of figures 5(c) and 5(d) show about the same trend of stability as for the basic wing, which was characterized by a rapid increase in stability before maximum lift followed by an abrupt instability near $C_{L_{max}}$. The pressure-distribution data of figure 11 indicate that immediately behind the peak negative pressure there is an extremely steep adverse pressure gradient and, in order to maintain any control of separation, a suction slot must be well forward in the region of the steep adverse pressure gradient. The flow diagrams (fig. 6(b)) show that suction through

the 0.025c slots did reduce the spanwise flow of the boundary layer in the region behind the slot but was ineffective in delaying the onset of leading-edge separation and tip stall.

In the attempt to reduce the tendency for trailing-edge separation, suction at the 0.40c slot, in addition to the 0.005c slots, did not provide any further improvement of the stability of the model in the high-lift range (fig. 5(b)) for the lower-flow-rate condition and was detrimental for the higher-flow-rate condition. It is probable, however, that the 0.005c and the 0.40c slots in combination may have functioned more effectively if the flow through each could have been controlled independently because there was evidence of outflow at the forward slot due to the over-all reduction of the plenum-chamber suction pressure whenever the 0.40c slots were in operation. The stalling patterns (fig. 6) for this slot combination were similar to that of the basic wing which showed predominant leading-edge stall.

Characteristics of the Wing with Split Flaps

The basic wing equipped with split flaps produced a maximum-lift coefficient of 1.05 (fig. 7) and the longitudinal stability characteristics are similar to those for the plain wing with the inherently abrupt instability occurring near $C_{L_{max}}$. Boundary-layer control at the 0.005c slot increased the maximum-lift coefficient to 1.12 and 1.21 at blower operating conditions of 3000 and 4000 rpm, respectively. With suction control employed, the longitudinal stability was improved in the low- and moderate-lift range, but near $C_{L_{max}}$ the pitching-moment characteristics were unstable. The tuft diagrams (fig. 8) and the surface pressures (fig. 12) show the flow pattern to be typical of that for the plain wing with and without boundary-layer control. The application of suction at the outboard half of the 0.005c slots with or without the additional 0.40c slots did not improve the lift or stability characteristics of the wing with split flaps.

Characteristics of the Wing with Extensible Leading-Edge Flaps

The maximum-lift coefficient of the wing with $0.47\frac{b}{2}$ leading-edge flaps without boundary-layer control was 1.13 (fig. 9(a)). Extending the flaps to $0.59\frac{b}{2}$ and $0.74\frac{b}{2}$ (figs. 9(b) and 9(c)) increased the maximum-lift coefficient to 1.18 in each case. The pitching-moment characteristics of the $0.47\frac{b}{2}$ and $0.59\frac{b}{2}$ leading-edge flaps were stable at the maximum lift but, for the $0.59\frac{b}{2}$ flaps leading edge, there was a tendency

for instability prior to the stable break at maximum lift. The flow diagrams of figure 10 indicate that initial stall occurred at the inboard end of the flaps as a result of the disturbance created by the plan-form discontinuity at the inboard end of the flap. The stable pitching moment at $C_{I_{max}}$ for the $0.47\frac{b}{2}$ and $0.59\frac{b}{2}$ leading-edge-flap configurations resulted from the combination of the clean-up of the tip flow and the growth of stall inboard. The airfoil surface pressures also show that the extensible leading-edge flaps eliminated the steep adverse pressure gradients and reduced the peak pressure coefficients which occurred for the plain wing (fig. 11) at each spanwise station covered by the flaps. When the flap span is increased to $0.74\frac{b}{2}$, a very stable curve was obtained prior to a very sharp unstable break at stall, which was characteristic of the stall of the plain wing. The increased stability near $C_{I_{max}}$ results from the loss of lift at the inboard sections where initial stall occurred. As the angle of attack is increased further, the control of the flow over the outboard sections is lost and tip stall predominated to produce abrupt instability.

The addition of boundary-layer suction at the 0.025c slots at the high flow rate produced no appreciable effects on the longitudinal stability of the model with either the $0.47\frac{b}{2}$ or the $0.59\frac{b}{2}$ leading-edge flaps. For the reduced suction-flow condition, however, there is indication of improvement in the stability near $C_{I_{max}}$. With suction at a high flow rate, higher lift was maintained over the outboard sections which produced the stabilizing pitching tendency prior to $C_{I_{max}}$, but stalling eventually progressed outward from the inboard end of the flap (fig. 10) and was not influenced by the suction, and this produced a momentary instability immediately before a stable stall. It is probable that suction at the lower flow rate did not control the separation at the tip so effectively which ultimately produced a smoother stable pitching-moment curve in the high-lift range.

Suction at the maximum flow rate provided stability to $C_{I_{max}}$ for the larger $0.74\frac{b}{2}$ leading-edge-flap configuration; however, it was not defined beyond this point. Suction at the lower flow rate was unable to delay tip stall and therefore instability occurred at $C_{I_{max}}$. The addition of suction at a high flow rate through the 0.40c slots, as well as the 0.025c slots for the $0.74\frac{b}{2}$ leading-edge-flap configuration, produced stability to maximum lift; however, it was not defined beyond this point. This combination also gave a maximum-lift coefficient of 1.29 which was the highest obtained for this configuration. The flow diagrams

of figure 10 indicate that the flow over the region behind the slots was greatly improved and the stall was restricted to the inboard sections of the wing. However, for the configuration with split flaps and $0.74\frac{b}{2}$ extensible leading-edge flaps (fig. 9(c)) in conjunction with suction resulted in a maximum-lift coefficient of 1.32, and longitudinal instability at $C_{L_{max}}$.

Effect of Power Failure

Suction-power failure with the slots open would reduce the maximum-lift coefficients of the plain wing and the wing with $0.74\frac{b}{2}$ extensible leading-edge flaps by 0.21 and 0.17, respectively, and the values of $C_{L_{max}}$ thus obtained are less than those for the sealed wing configurations (fig. 16). The measured drag in the low-lift range was essentially unaffected for the slots-open fan-inoperative condition but, at a C_L of 0.3 or 0.5, depending upon the flap configuration, the drag for the fan-inoperative condition increased rapidly. In the high angle-of-attack range near $C_{L_{max}}$ the effect of suction failure is to increase the drag coefficient about 0.120 which, for the flap-deflected configuration, represents over a 50-percent drag increase. Except for the reduction in the maximum-lift coefficient, the sudden loss in the suction power on the plain wing and the 0.005c slots installed would not decrease the stability or introduce instability at stall, although a small trim shift would occur. For the wing with the $0.74\frac{b}{2}$ leading-edge flaps and the 0.025c slots the sudden power failure would be appreciably more serious. For operation near $C_{L_{max}}$ there would be a large trim shift and a recurrence of instability as a result of the loss in lift over the tip sections. In the event of suction-power failure, it would be advisable to have a device whereby outflow would be eliminated.

Drag Coefficients

Boundary-layer control at the leading edge reduced the measured external drag coefficients in the high-lift range but did not appreciably change the drag in the low- and moderate-lift range.

The drag coefficients presented in the data figures, as has been noted, do not include the blower-power drag coefficients and, if it is of interest to determine the total-drag coefficients for the conditions with boundary-layer control, the drag coefficient equivalent to the

power required to discharge the air removed from the boundary layer at free-stream total head must be included. (See reference 8.) It is apparent that leading-edge suction slots located in a region of high negative pressures would produce fairly high-power drag coefficients.

SUMMARY OF RESULTS

The results of the investigation in the Langley full-scale tunnel of the effects of leading-edge boundary-layer suction with high-lift devices on the aerodynamic characteristics of a 47.5° sweptback wing are summarized as follows:

1. Change in Reynolds number from 3.0×10^6 to 7.5×10^6 and from 3.0×10^6 to 6.1×10^6 for the plain wing and the wing with split flaps, respectively, had no appreciable effects on the lift and drag characteristics of the model. The abrupt instability which occurred at initial stall was progressively shifted to higher lift coefficients between Reynolds numbers of 3.0×10^6 and 5.2×10^6.

2. The maximum-lift coefficient of the plain wing without boundary-layer control was 1.03. Applying suction at the maximum flow rate at the 0.005-chord slots or at the 0.025-chord slots increased the maximum-lift coefficient to about 1.20. The model was longitudinally stable at the maximum lift for the 0.73-percent span 0.005-chord slot configuration although a slight instability occurred prior to the stall. Suction applied along the outboard 50 percent of the wing span of the 0.005-chord slots resulted in static longitudinal stability through the lift range and at a maximum-lift coefficient of 1.13.

3. The maximum-lift coefficients of the wing with split flaps, with and without boundary-layer suction, were of the same magnitude as the plain wing and suction did not improve the longitudinal stability characteristics of the model.

4. The 0.47 semispan, 0.59 semispan, and 0.74 semispan extensible leading-edge flaps, combined with suction at the 0.025-chord slot, produced small increments in maximum lift of 0.06, 0.03, and 0.08 resulting in maximum-lift coefficients of 1.19, 1.21, and 1.26, respectively. The smaller-span leading-edge-flap configuration was longitudinally stable near maximum lift for the conditions with and without suction but for the 0.74-percent-span-flap configuration, longitudinal stability near the maximum lift was attained only with a high-suction-flow rate. The highest value of maximum-lift coefficient obtained in this investigation was 1.32 for the wing with the 0.74-percent-span flaps in combination with the split flaps and boundary-layer suction but the wing was unstable at stall.

5. Blower-power failure would result in a reduction of the maximum-lift coefficients and instability at the stall for the leading-edge-flap configuration.

Langley Aeronautical Laboratory
National Advisory Committee for Aeronautics
Langley Air Force Base, Va.

REFERENCES

1. Graham, Robert R., and Conner, D. William: Investigation of High-Lift and Stall-Control Devices on an NACA 64-Series 42° Sweptback Wing with and without Fuselage. NACA RM L7G09, 1947.

2. Quinn, John H., Jr.: Tests of the NACA 64_1A212 Airfoil Section with a Slat, a Double Slotted Flap, and Boundary-Layer Control by Suction. NACA TN 1293, 1947.

3. Nuber, Robert J., and Needham, James R., Jr.: Exploratory Wind-Tunnel Investigation of the Effectiveness of Area Suction in Eliminating Leading-Edge Separation over an NACA 64_1A212 Airfoil. NACA TN 1741, 1948.

4. Pasamanick, Jerome, and Proterra, Anthony J.: The Effect of Boundary-Layer Control by Suction and Several High-Lift Devices on the Longitudinal Aerodynamic Characteristics of a 47.5° Sweptback Wing-Fuselage Combination. NACA RM L8E18, 1948.

5. McCullough, George B., and Gault, Donald E.: An Experimental Investigation of an NACA 63_1-012 Airfoil Section with Leading-Edge Suction Slots. NACA TN 1683, 1948.

6. Theodorsen, Theodore, and Silverstein, Abe: Experimental Verification of the Theory of Wind-Tunnel Boundary Interference. NACA Rep. 478, 1934.

7. Lange, Roy H., Whittle, Edward F., Jr., and Fink, Marvin P.: Investigation at Large Scale of the Pressure Distribution and Flow Phenomena over a Wing with the Leading Edge Swept Back 47.5° Having Circular-Arc Airfoil Sections and Equipped with Drooped-Nose and Plain Flaps. NACA RM L9G15, 1949.

8. Burrows, Dale L., Braslow, Albert L., and Tetervin, Neal: Experimental and Theoretical Studies of Area Suction for the Control of the Laminar Boundary Layer on a Porous Bronze NACA 64A010 Airfoil. NACA TN 1905, 1949.

TABLE I

AIRFOIL ORIFICE LOCATION

Chordwise station, x/c'	
Upper surface	Lower surface
0	0
.005	.005
.010	.010
.015	.015
.025	.025
.040	.040
.060	----
.080	----
.120	----
.170	.170
.220	----
.320	.320
.420	----
.520	.520
.620	----
.720	.720

NACA

TABLE II

SUMMARY OF MAXIMUM-LIFT RESULTS AND LONGITUDINAL STABILITY CHARACTERISTICS

Configuration	Suction slots	Suction-flow rate	$C_{L_{max}}$	$\Delta C_{L_{max}}$ (suction)	Stability C_m against C_L	Figure
Plain wing	Sealed	--------	1.03	----		5(a)
	0.005c	High	1.20	0.17		5(a)
	0.005c	Moderate	1.12	.09		5(a)
	0.005c	Suction power failure	.98	-.21		16(a)
	Outboard 0.005c	High	1.13	.10		5(a)
	0.005c and 0.40c	High	1.19	.16		5(b)
	0.005c and 0.40c	Moderate	1.13	.10		5(b)
	Outboard 0.005c and 0.40c	High	1.17	.14		5(b)
	0.025c	High	1.20	.17		5(c)
	0.025c	Moderate	1.13	.10		5(c)
	0.025c and 0.40c	High	1.19	.16		5(d)
	0.025c and 0.40c	Moderate	1.13	.10		5(d)
Semispan split flaps	Sealed	--------	1.06	----		7(a)
	0.005c	High	1.22	.16		7(a)
	0.005c	Moderate	1.13	.07		7(a)
	Outboard 0.005c	High	1.18	.12		7(a)
	0.005c and 0.40c	High	1.20	.14		7(b)
	0.005c and 0.40c	Moderate	1.11	.05		7(b)
	Outboard 0.005c and 0.40c	High	1.20	.14		7(b)

TABLE II.- Concluded

SUMMARY OF MAXIMUM-LIFT RESULTS AND LONGITUDINAL STABILITY CHARACTERISTICS - Concluded

Configuration	Suction slots	Suction-flow rate	$C_{L_{max}}$	$\Delta C_{L_{max}}$ (suction)	Stability C_m against C_L	Figure
Extensible leading-edge flaps - $0.47\frac{b}{2}$	Sealed	--------	1.13	----		9(a)
	0.025c	High	1.19	0.06		9(a)
	0.025c	Moderate	1.17	.04	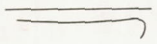	9(a)
$0.59\frac{b}{2}$	Sealed	--------	1.18	----		9(b)
	0.025c	High	1.21	.03		9(b)
	0.025c	Moderate	1.20	.02		9(b)
$0.74\frac{b}{2}$	Sealed	--------	1.18	----		9(c)
	0.025c	High	1.26	.08		9(c)
	0.025c	Moderate	1.23	.05		9(c)
	0.025c	Suction power failure	1.09	-.17		16(b)
	0.025c and 0.40c	High	1.29	.11		9(d)
	0.025c and 0.40c	Moderate	1.24	.06		9(d)
$0.74\frac{b}{2}$ and semispan split flaps	0.025c	High	1.32	----	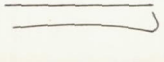	9(c)

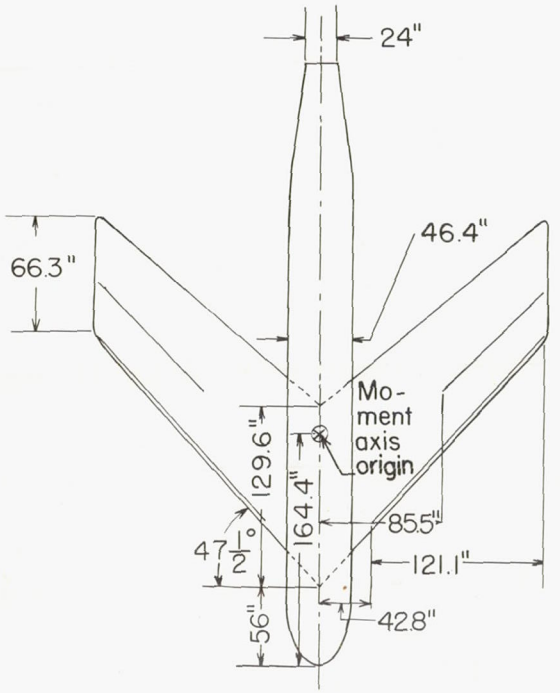

Wing area	225.98 sq ft
Aspect ratio	3.4
Taper ratio	0.51
Airfoil section	NACA 64_1A112
Root chord	10.8 ft
Tip chord	5.5 ft
$\bar{c}$	8.78 ft

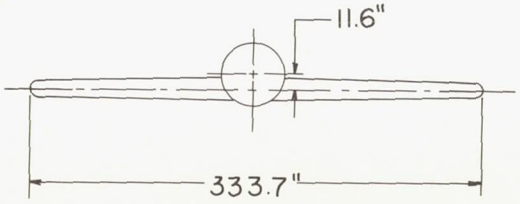

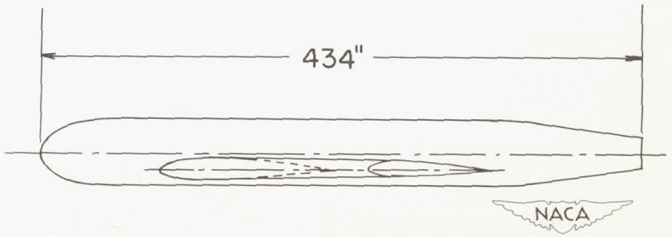

Figure 1.- Three-view drawing of a 47.5° sweptback wing-fuselage combination with boundary-layer control.

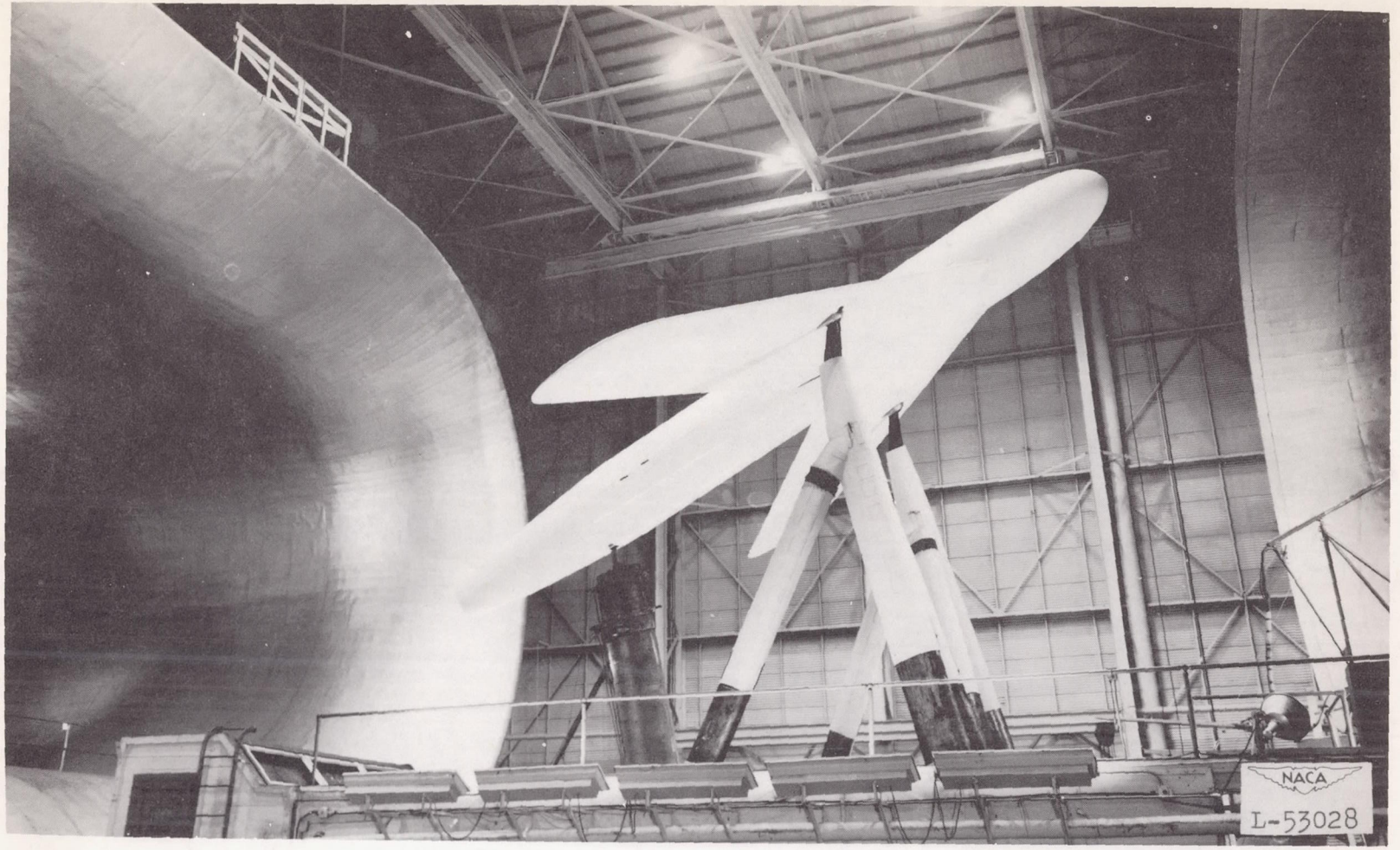

Figure 2.- Three-quarter front view of the 47.5° sweptback wing boundary-layer-control model mounted in the Langley full-scale tunnel.

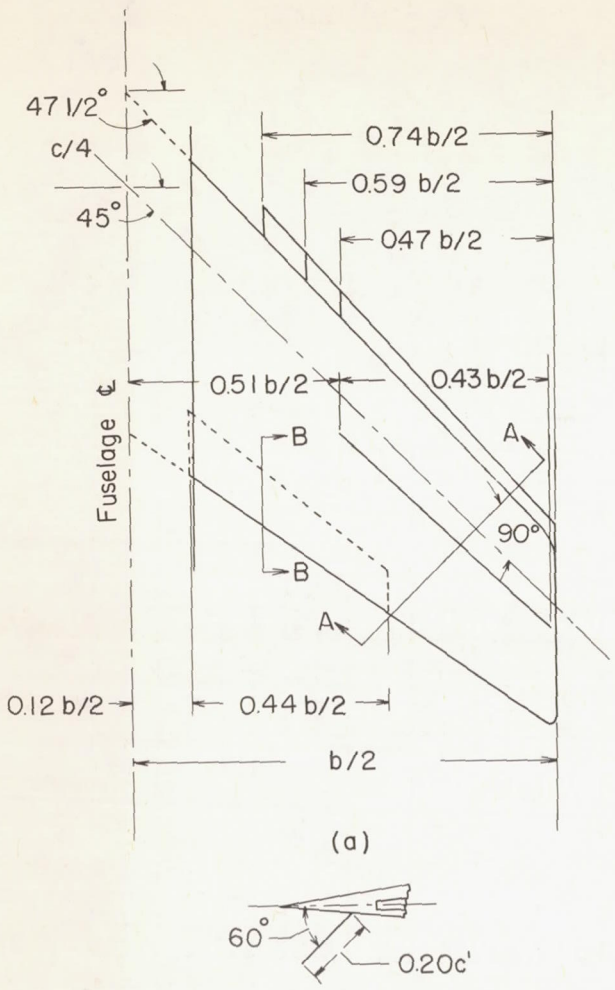

(a)

(c) Section BB.

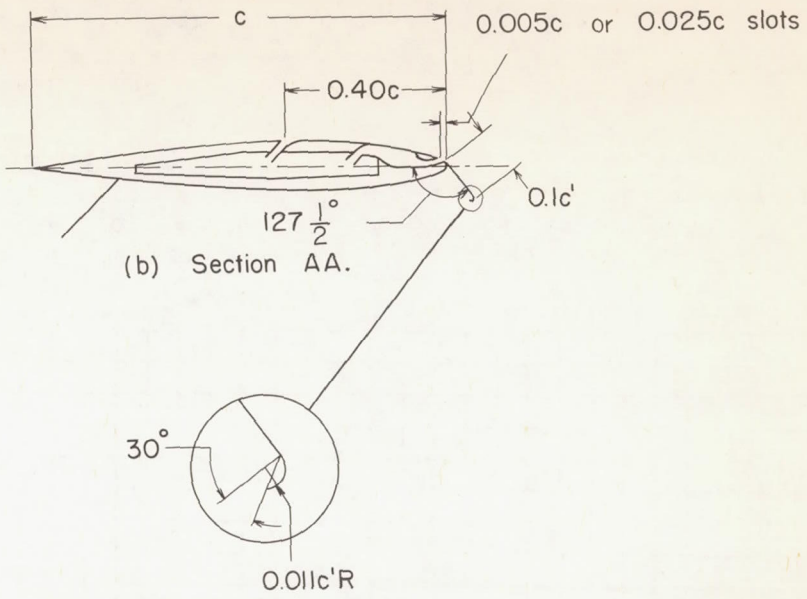

(b) Section AA.

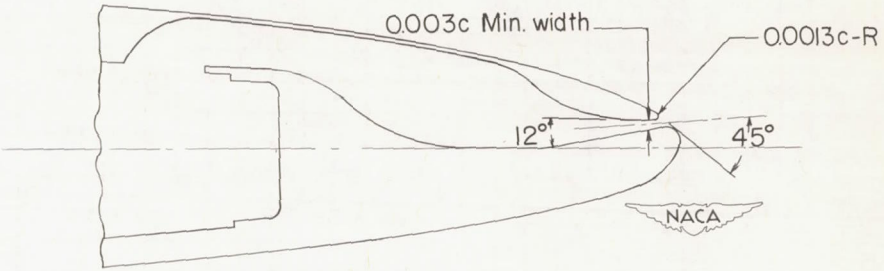

(d) Enlarged view of leading-edge suction slot.

Figure 3.- The location and detail dimensions of high-lift devices.

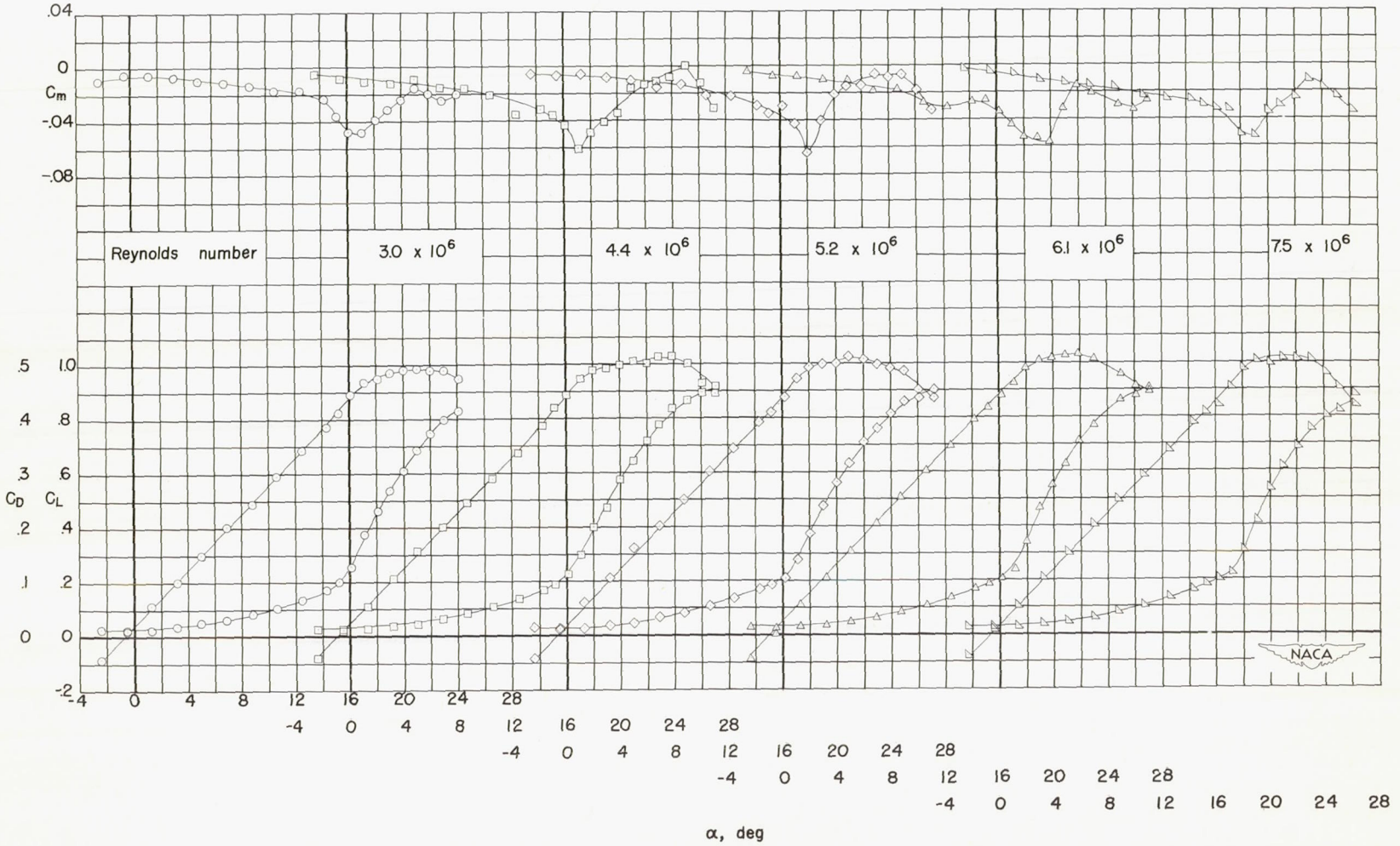

(a) Plain wing.

Figure 4.- Effect of Reynolds number on the aerodynamic characteristics of a 47.5° sweptback wing-fuselage combination. Suction slots sealed and faired.

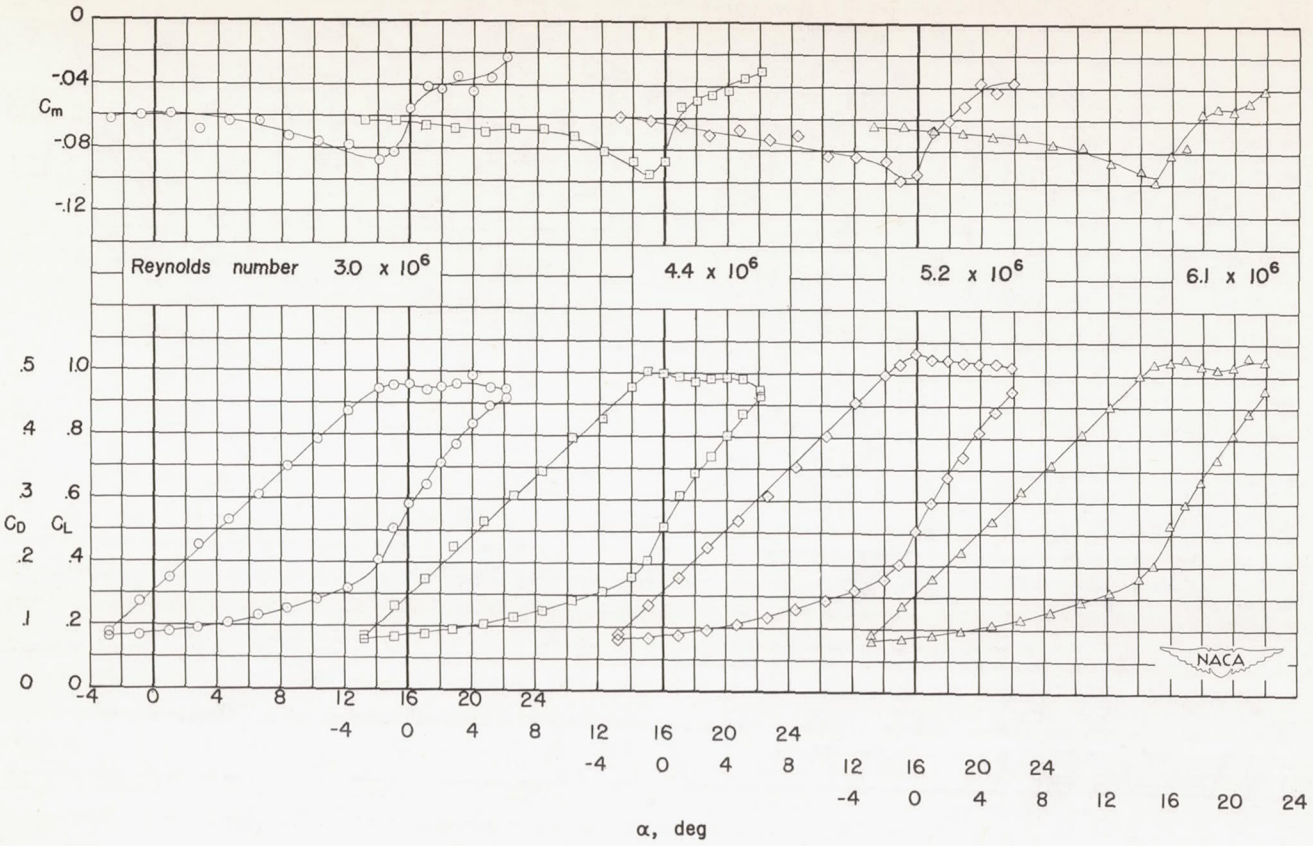

(b) Semispan split flaps.

Figure 4.- Concluded.

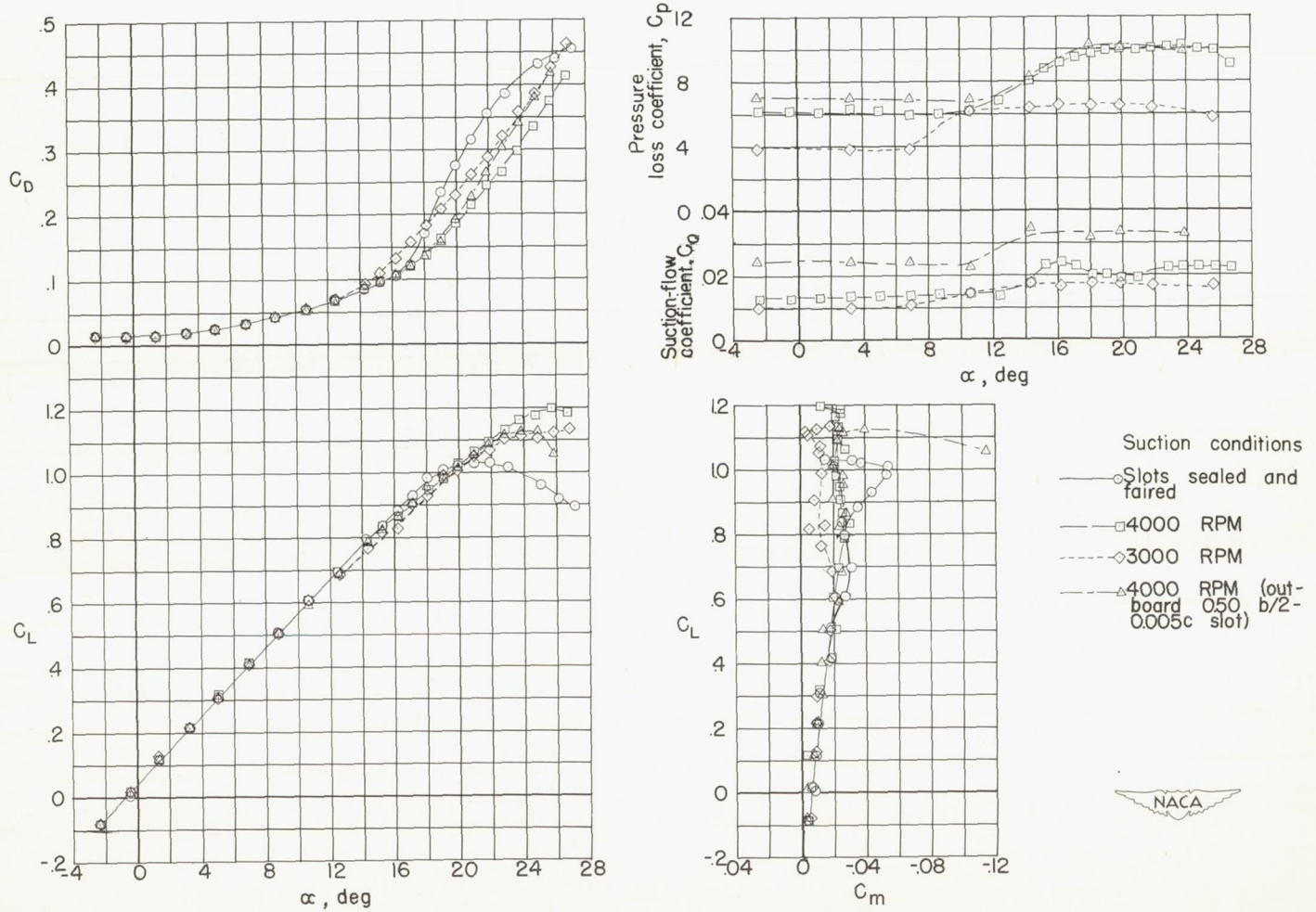

(a) 0.005c slots $\left(0.73\frac{b}{2}\right)$.

Figure 5.- Effect of boundary-layer control by suction on the aerodynamic characteristics of a 47.5° sweptback wing-fuselage combination. $R = 6.1 \times 10^6$.

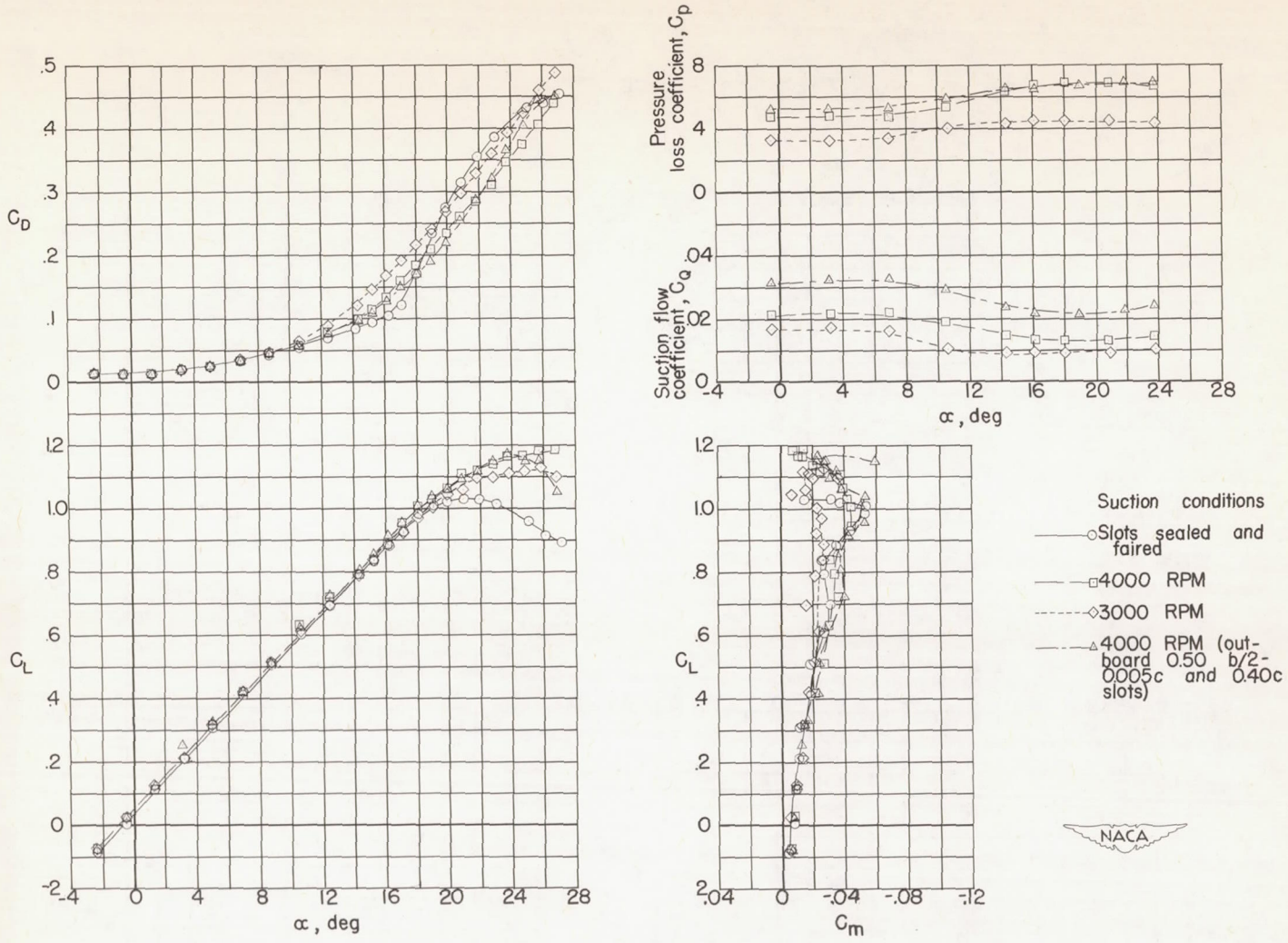

(b) 0.005c slots $\left(0.73\frac{b}{2}\right)$ and 0.40c slots.

Figure 5.- Continued.

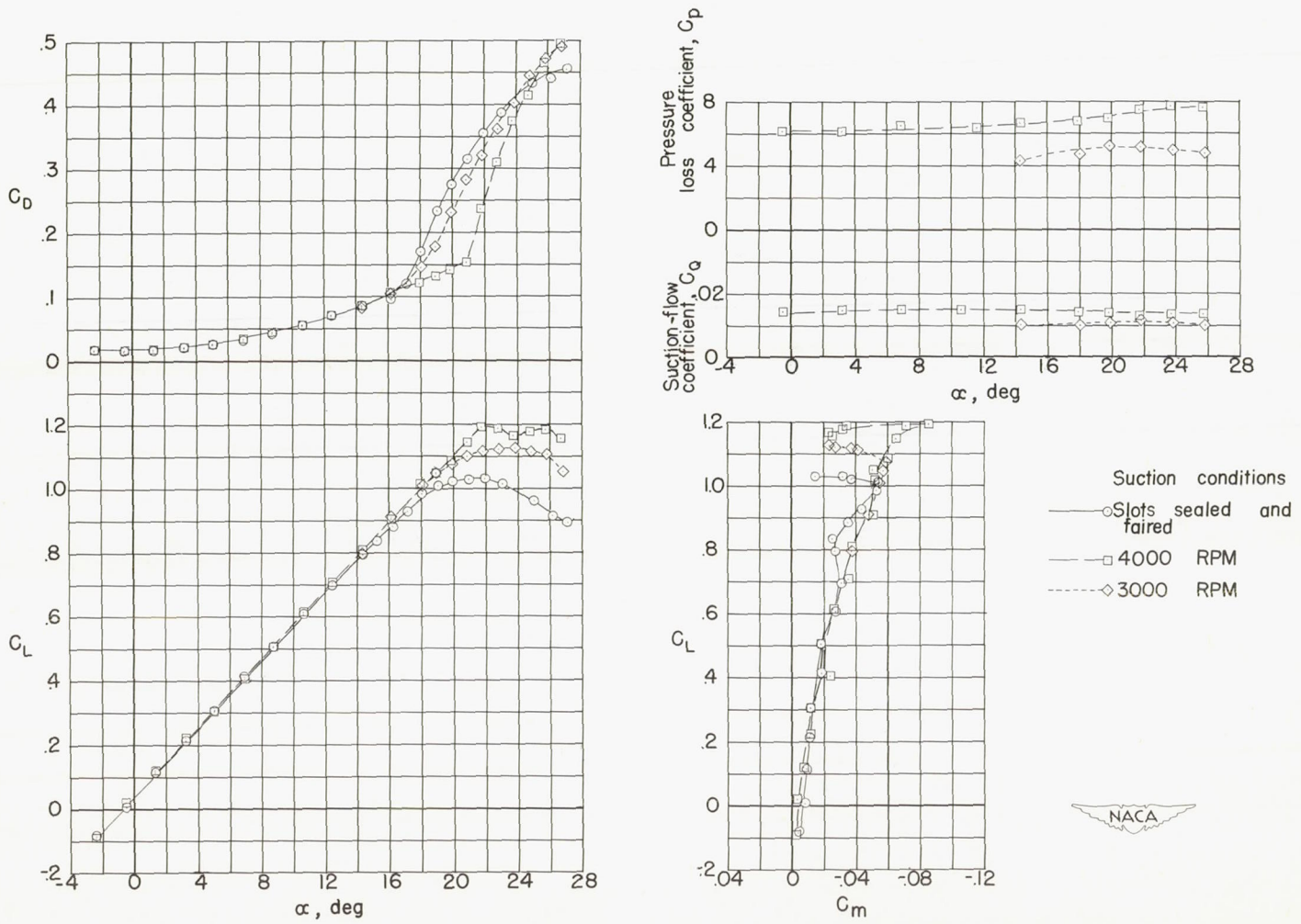

(c) 0.025c slots $\left(0.73\frac{b}{2}\right)$.

Figure 5.- Continued.

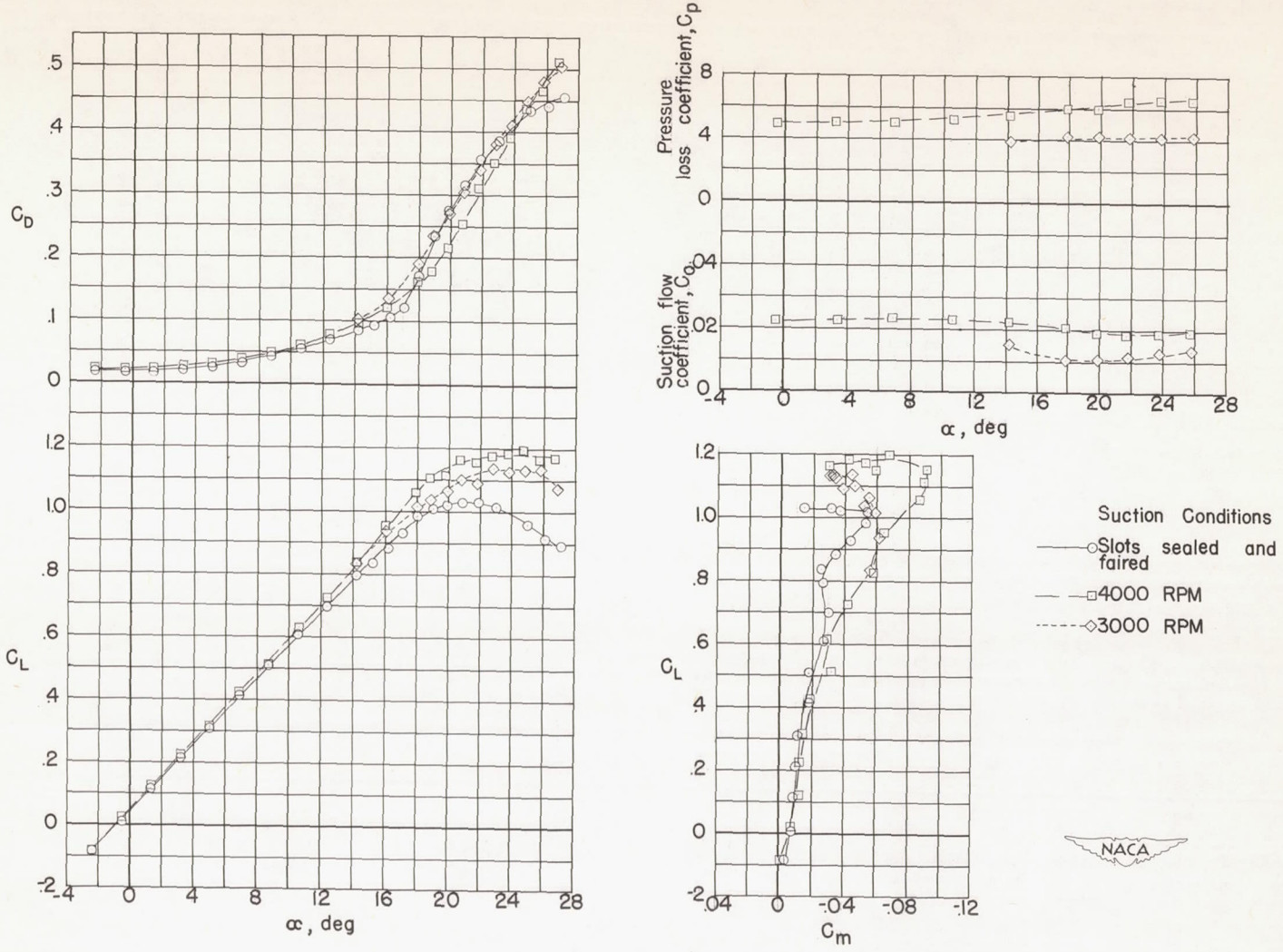

(d) 0.025c slots $\left(0.73\frac{b}{2}\right)$ and 0.40c slots.

Figure 5.- Concluded.

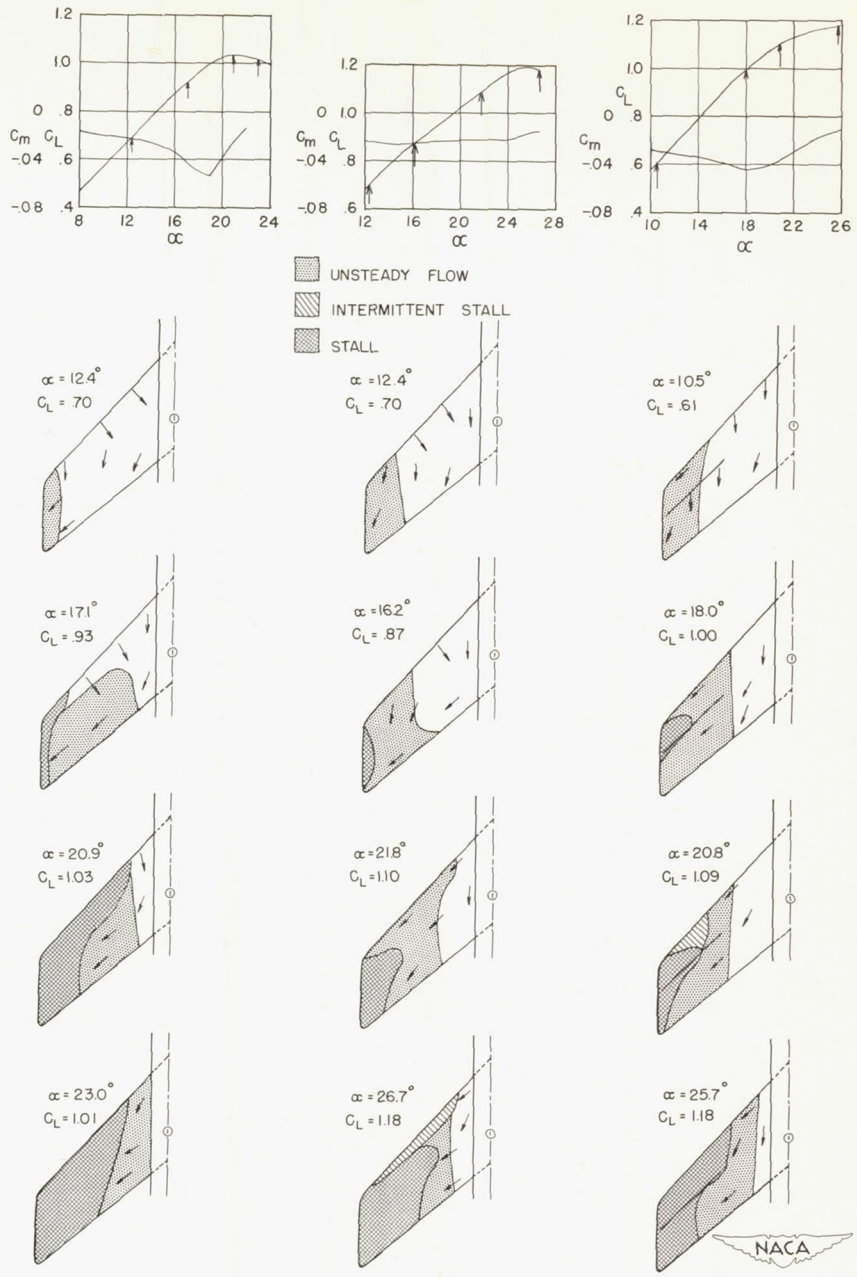

Slots sealed and faired.

Suction at 0.005c slots $\left(0.73\frac{b}{2}\right)$ 4000 rpm.

Suction at 0.005c slots $\left(0.73\frac{b}{2}\right)$ and 0.40c slots, 4000 rpm.

(a) 0.005c slots $\left(0.73\frac{b}{2}\right)$.

Figure 6.- Stalling characteristics of a 47.5° sweptback wing-fuselage combination with and without suction. $R = 6.1 \times 10^6$.

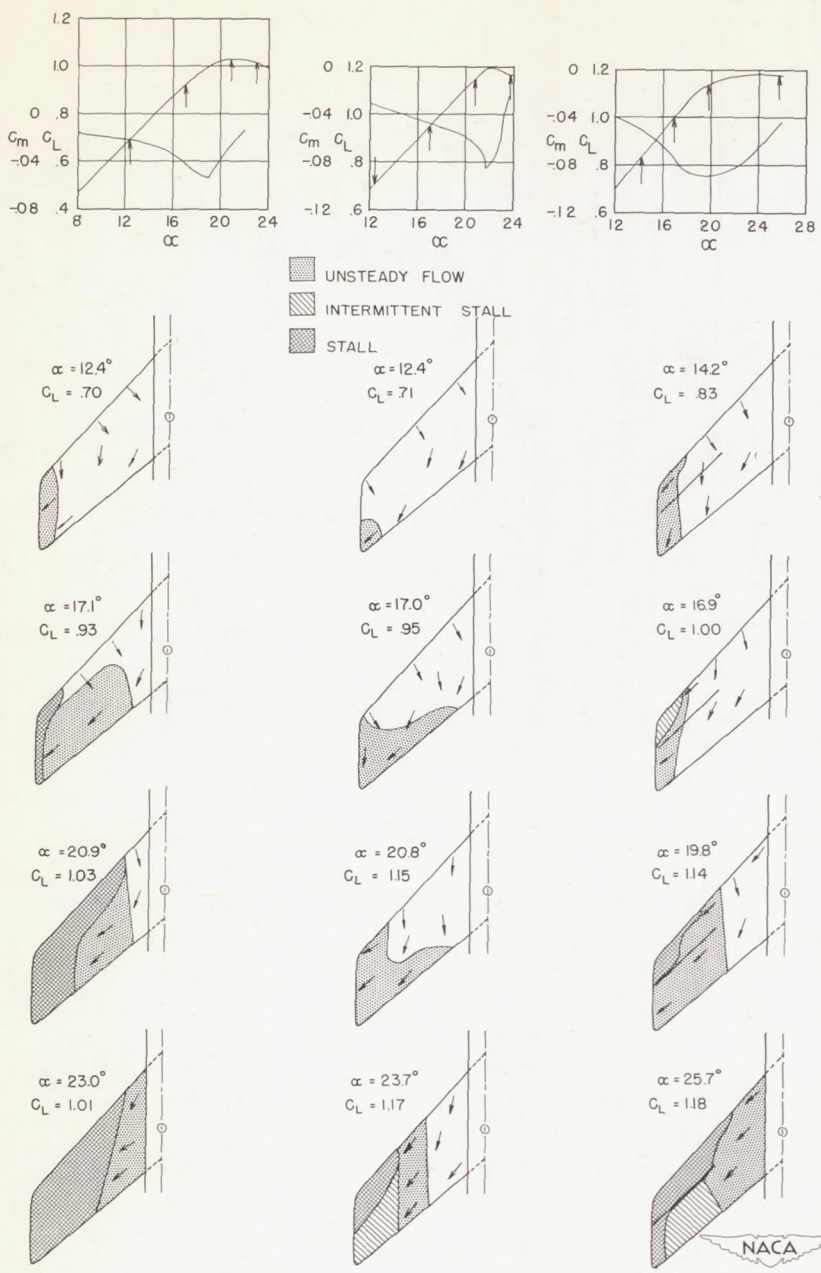

Slots sealed and faired.

Suction at 0.025c slots $\left(0.73\frac{b}{2}\right)$ 4000 rpm.

Suction at 0.025c slots $\left(0.73\frac{b}{2}\right)$ and 0.40c slots, 4000 rpm.

(b) 0.025c slots $\left(0.73\frac{b}{2}\right)$.

Figure 6.- Concluded.

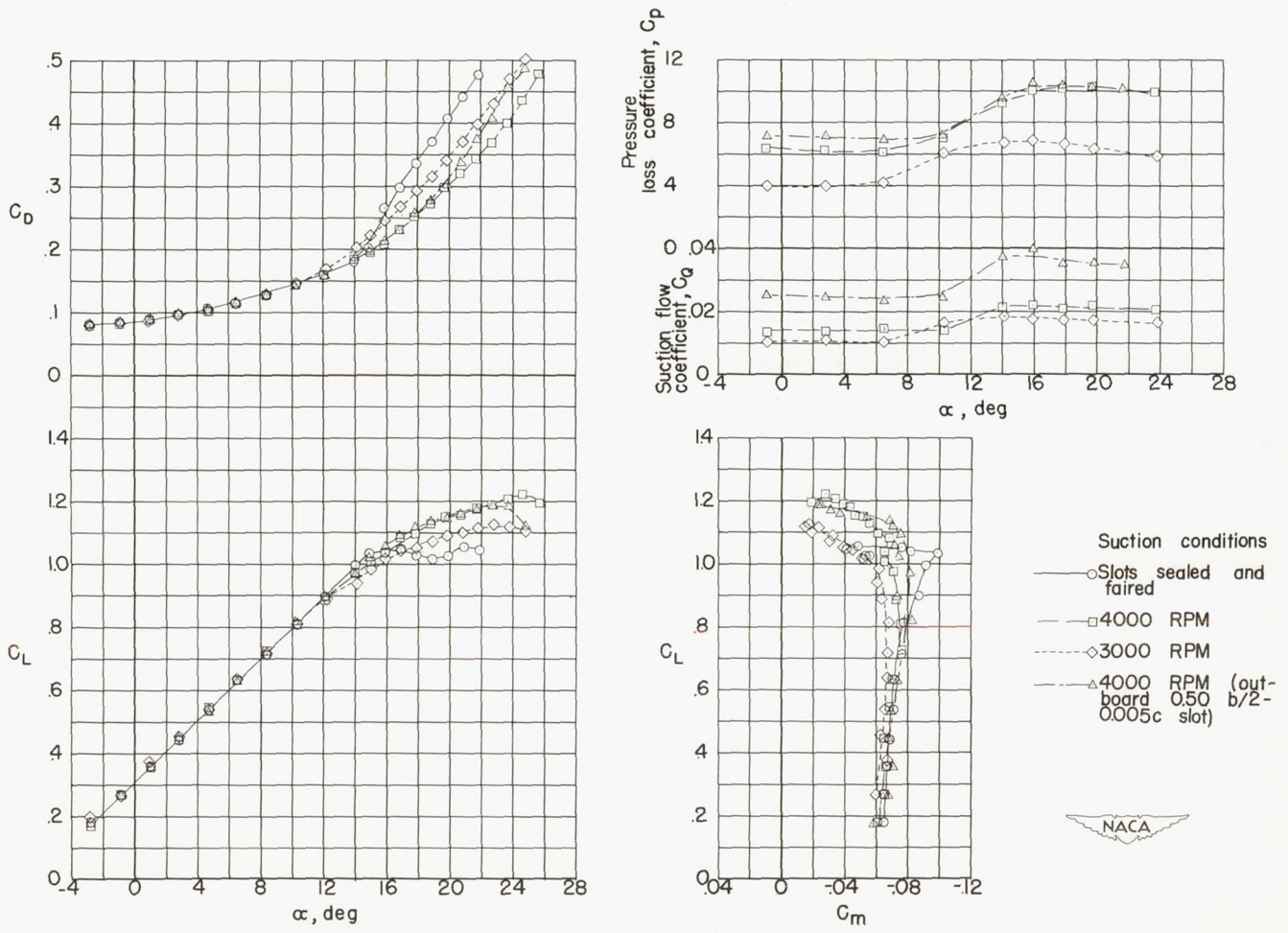

(a) 0.005c slots $\left(0.73\frac{b}{2}\right)$.

Figure 7.- Effect of boundary-layer control by suction on the aerodynamic characteristics of a 47.5° sweptback wing-fuselage combination with semispan split flaps. $R = 6.1 \times 10^6$.

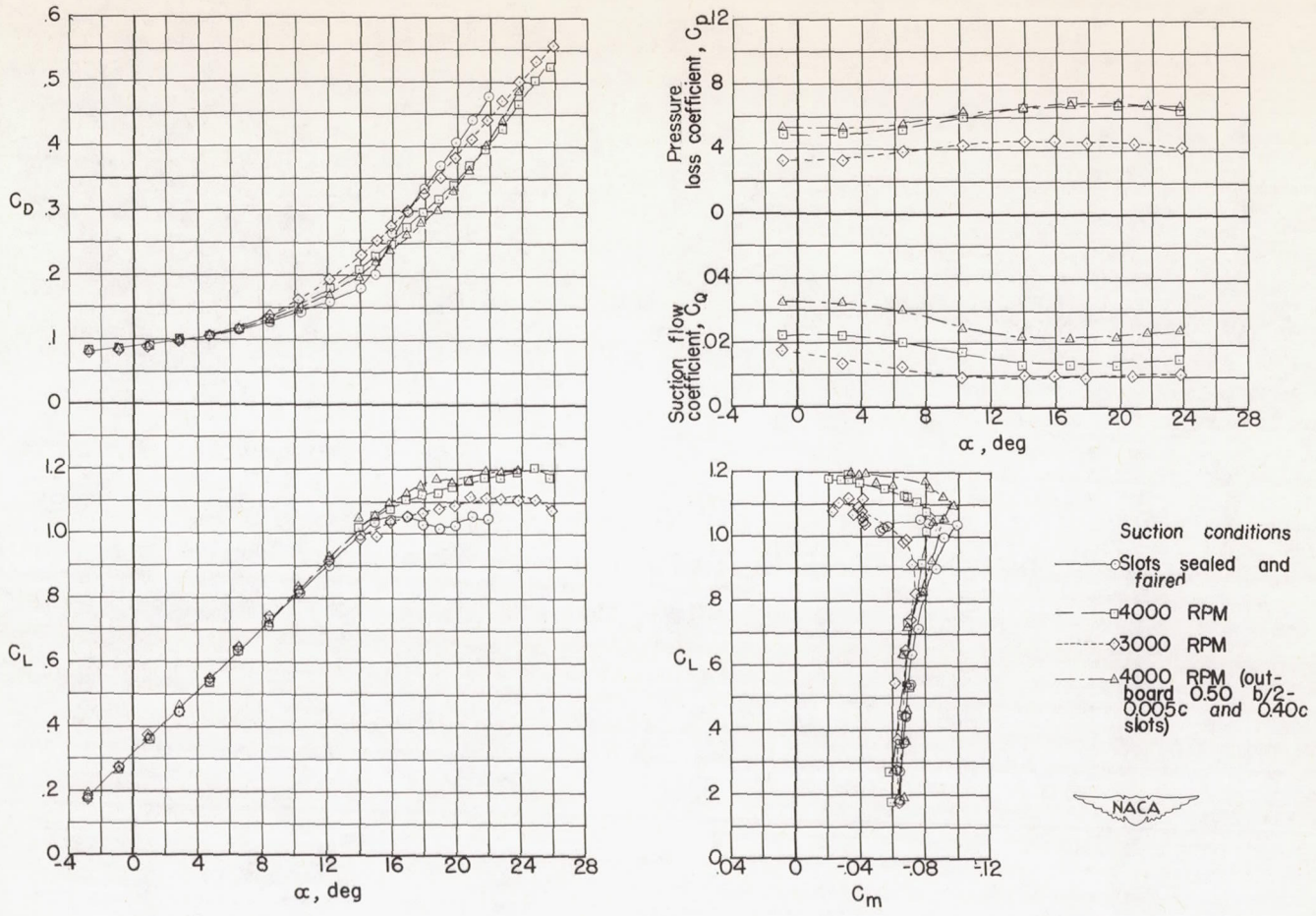

(b) 0.005c slots $\left(0.73\frac{b}{2}\right)$ and 0.40c slots.

Figure 7.- Concluded.

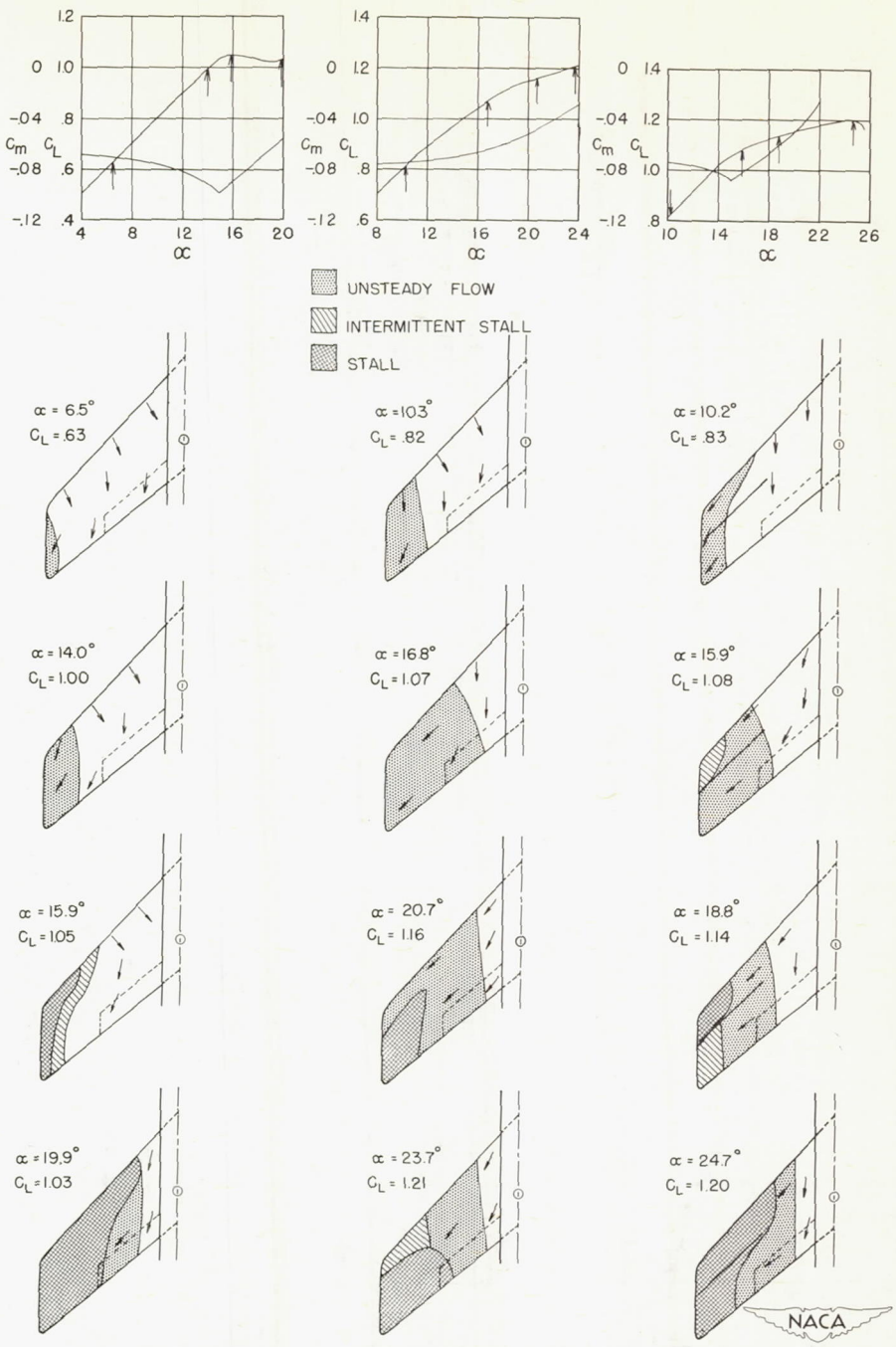

Slots sealed and faired.

Suction at 0.005c slots $\left(0.73\frac{b}{2}\right)$ 4000 rpm.

Suction at 0.005c slots $\left(0.73\frac{b}{2}\right)$ and 0.40c slots, 4000 rpm.

Figure 8.- Effect of semispan split flaps on the stalling characteristics of a 47.5° sweptback wing-fuselage combination with and without suction. $R = 6.1 \times 10^6$.

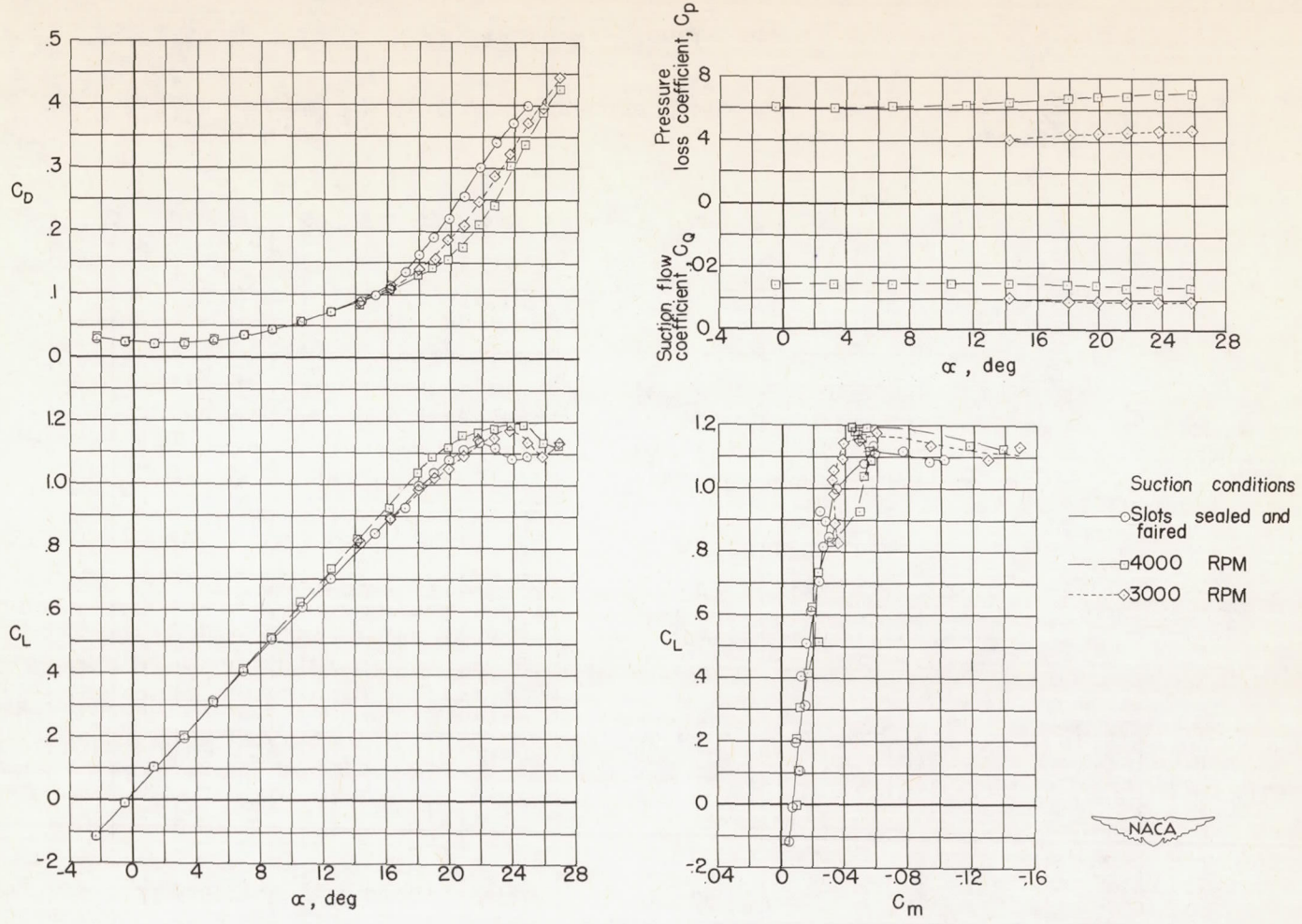

(a) $0.47\frac{b}{2}$ extensible leading-edge flaps. 0.025c slots $\left(0.73\frac{b}{2}\right)$.

Figure 9.- Effect of boundary-layer control by suction on the aerodynamic characteristics of a 47.5° sweptback wing-fuselage combination with extensible leading-edge flaps. R = 6.1×10^6.

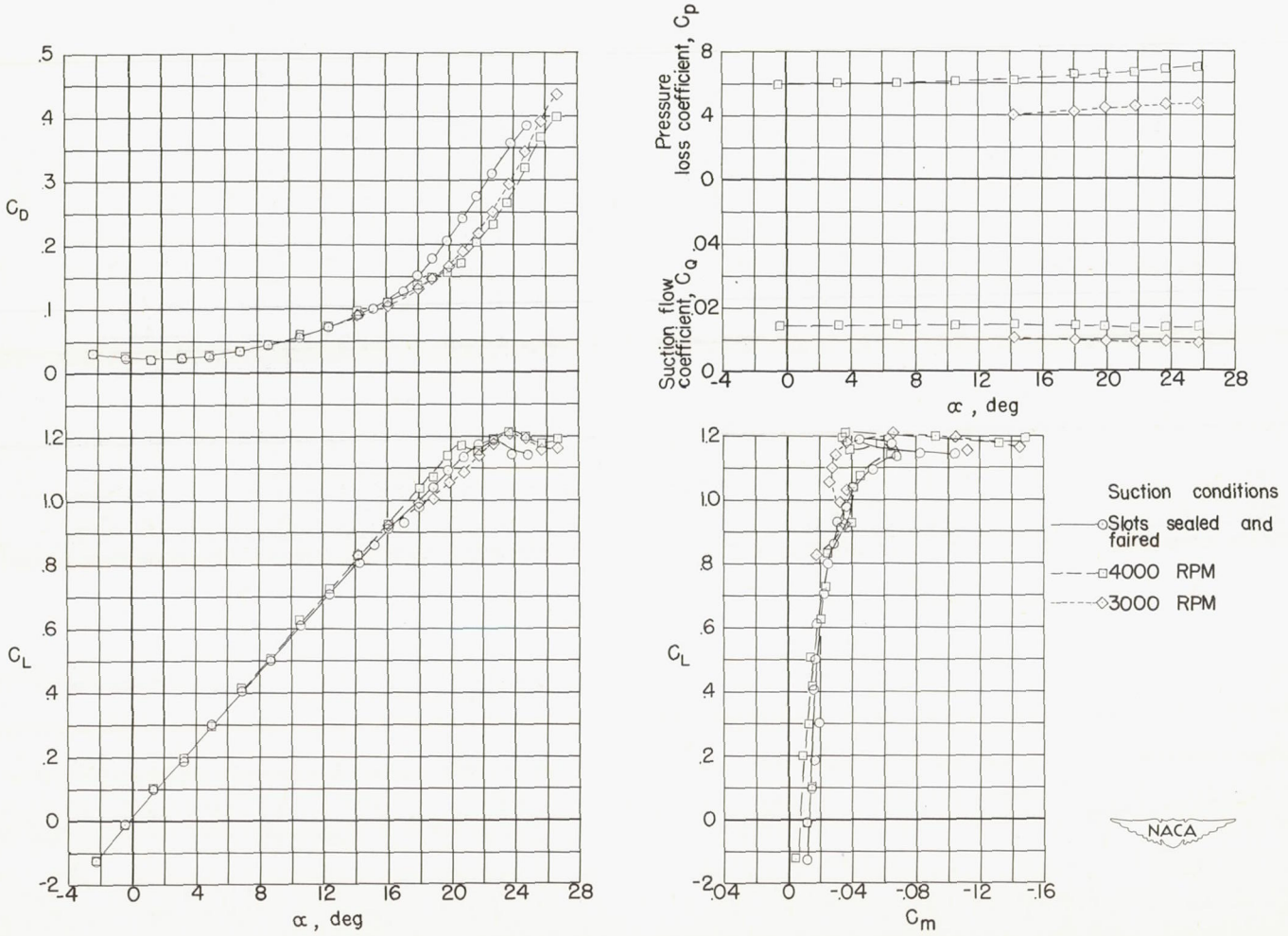

(b) $0.59\frac{b}{2}$ extensible leading-edge flaps. 0.025c slots $\left(0.73\frac{b}{2}\right)$.

Figure 9.- Continued.

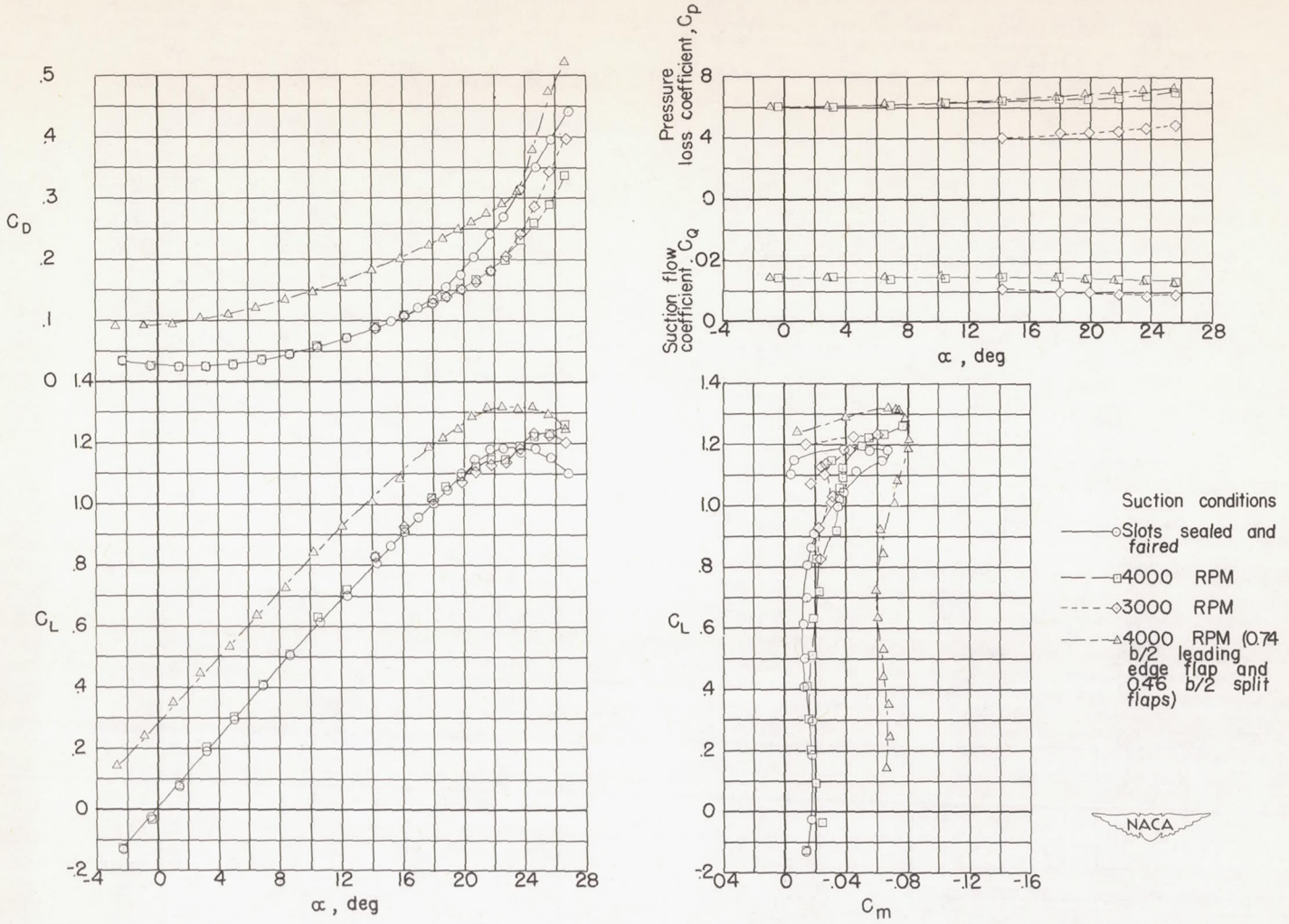

(c) $0.74\frac{b}{2}$ extensible leading-edge flaps. 0.025c slots $\left(0.73\frac{b}{2}\right)$.

Figure 9.- Continued.

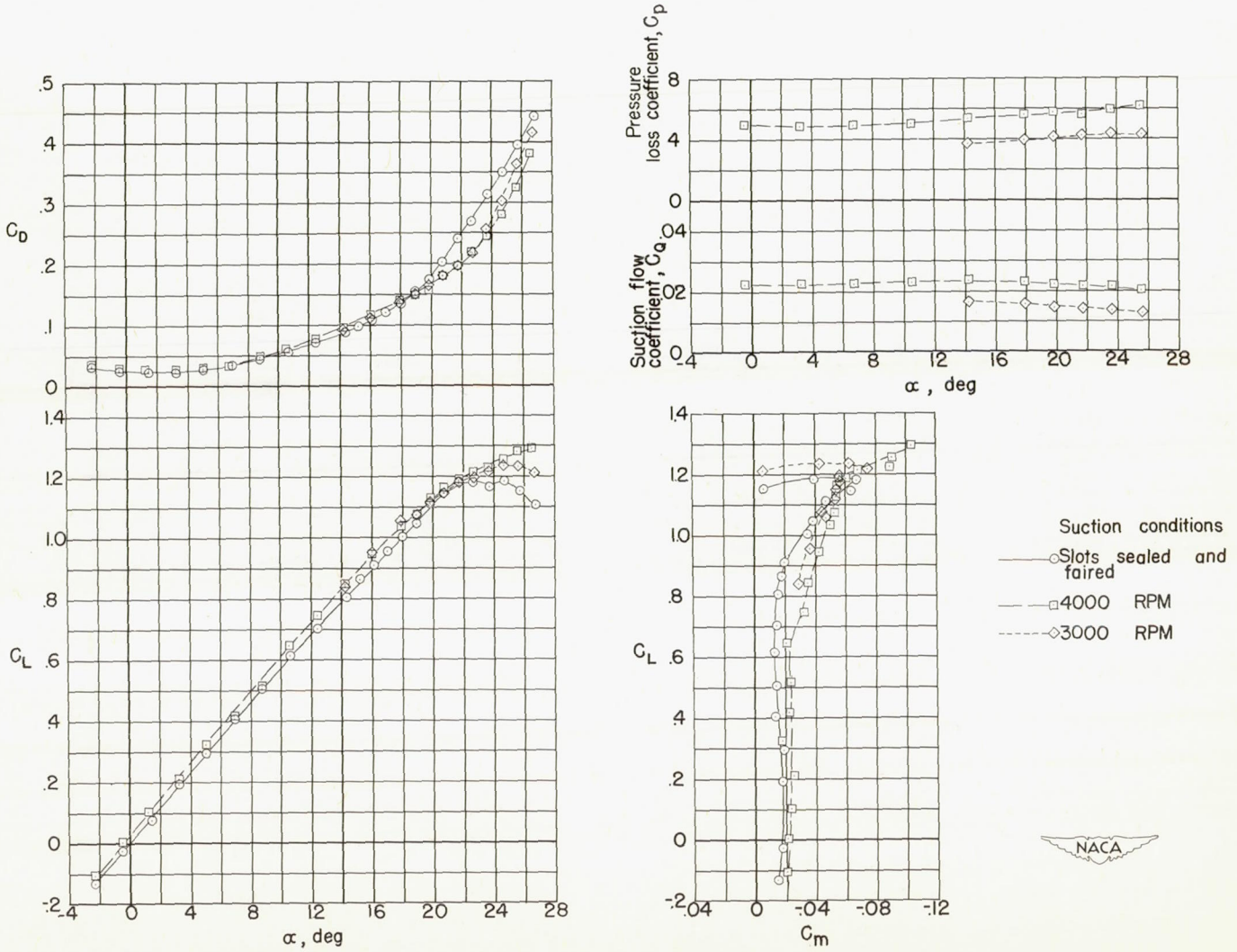

(d) $0.74\frac{b}{2}$ extensible leading-edge flaps. 0.025c slots $\left(0.73\frac{b}{2}\right)$ and 0.40c slots.

Figure 9.- Concluded.

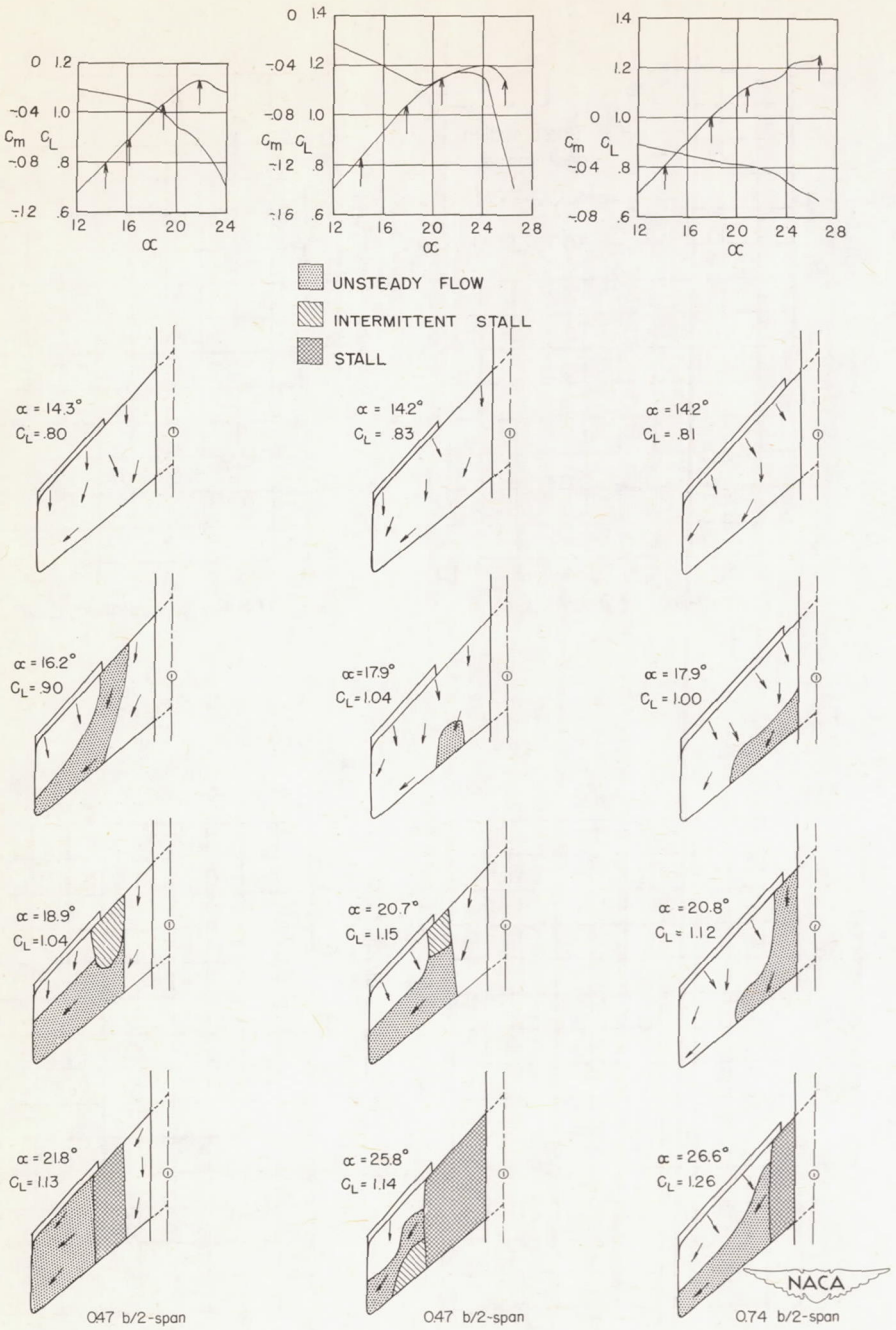

Slots sealed and faired.

Suction at 0.025c slots $\left(0.73\frac{b}{2}\right)$ 4000 rpm.

Suction at 0.025c slots $\left(0.73\frac{b}{2}\right)$ 4000 rpm.

Figure 10.- Effect of extensible leading-edge flaps on the stalling characteristics of a 47.5° sweptback wing-fuselage combination with and without suction. $R = 6.1 \times 10^6$.

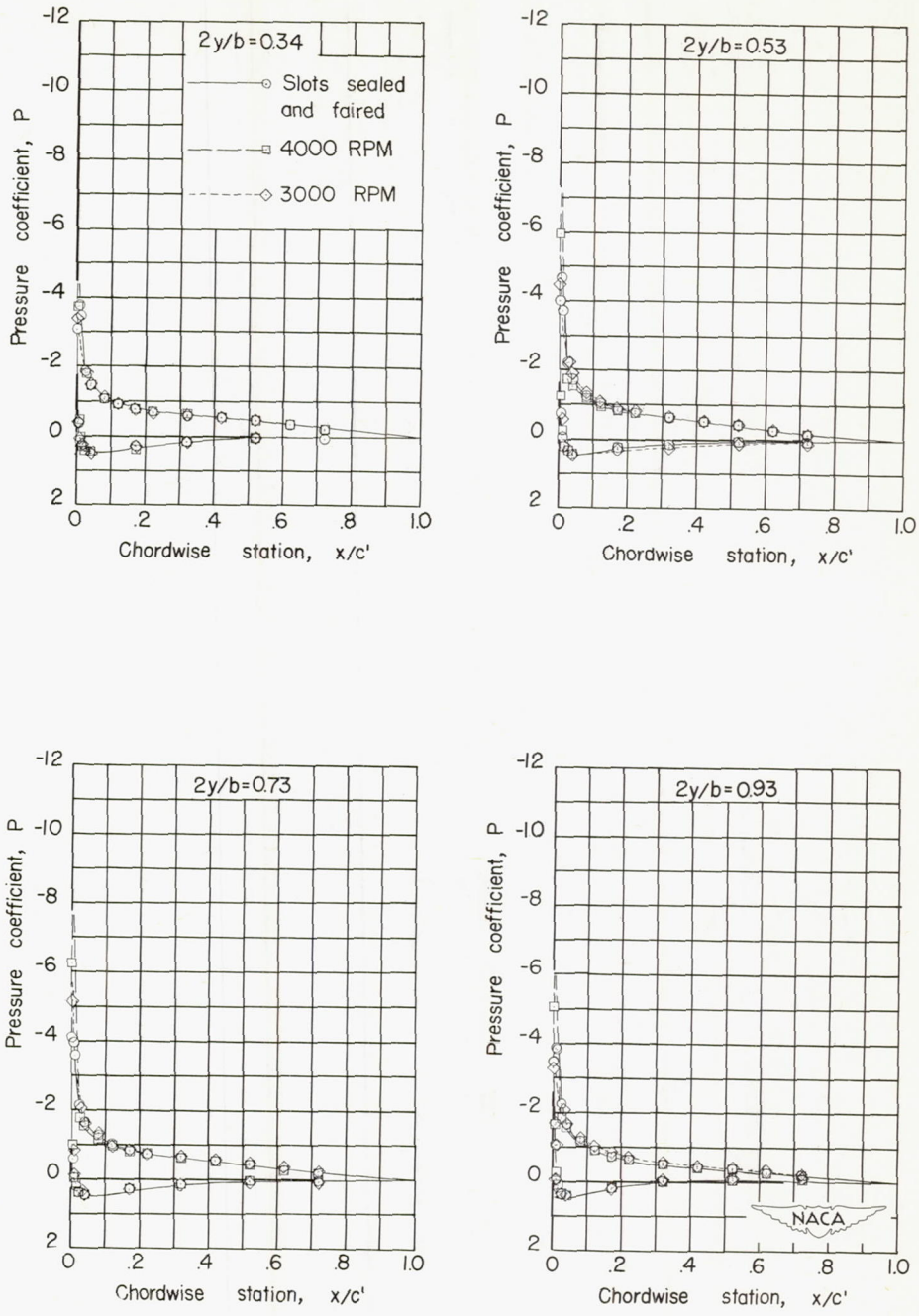

(a) $\alpha = 10.6^{\circ}$.

Figure 11.- Airfoil pressure distribution over a 47.5° sweptback wing with and without boundary-layer control. 0.005c slots $\left(0.73\frac{b}{2}\right)$. $R = 6.1 \times 10^{6}$.

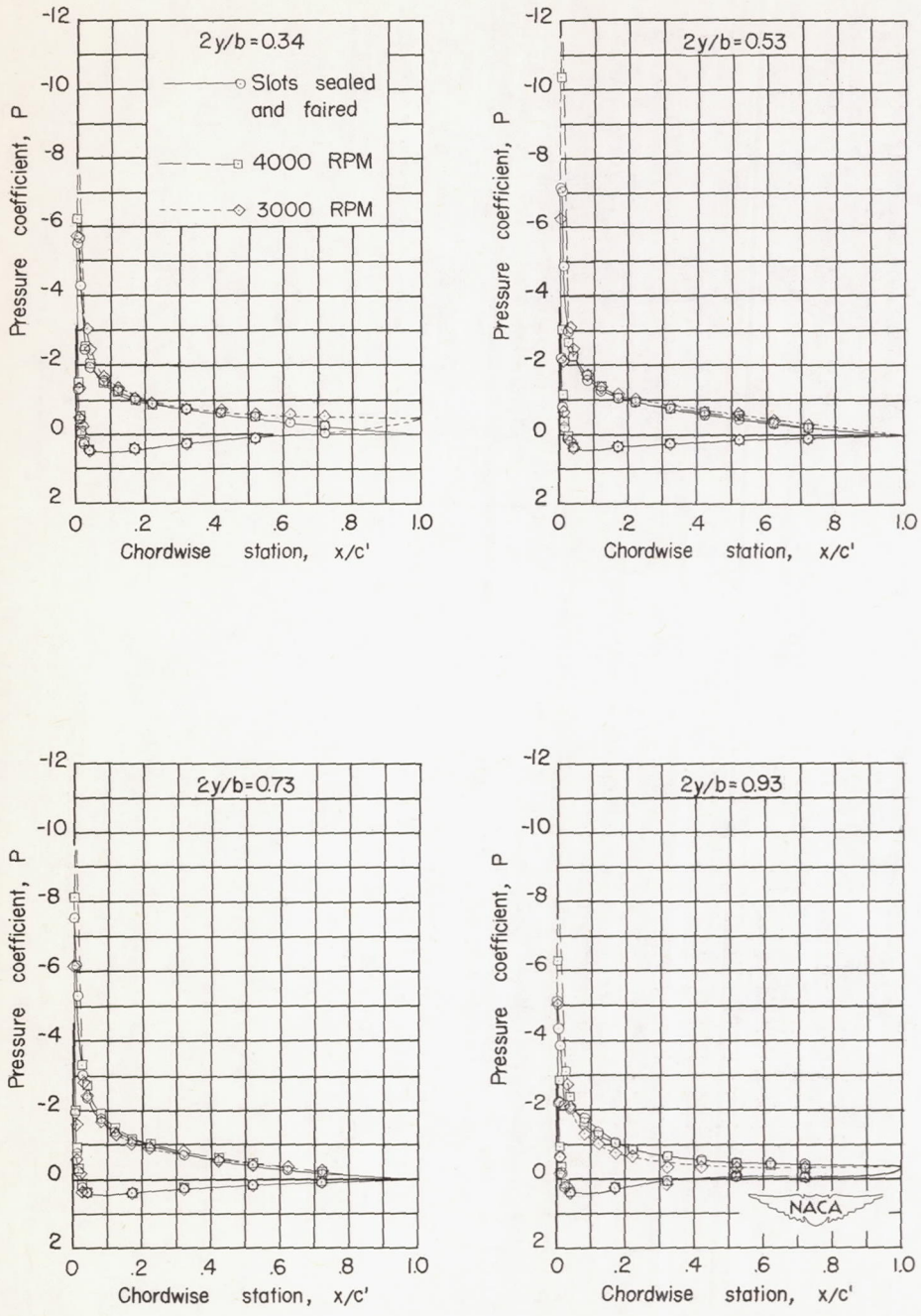

(b) $\alpha = 14.3^{\circ}$.

Figure 11.- Continued.

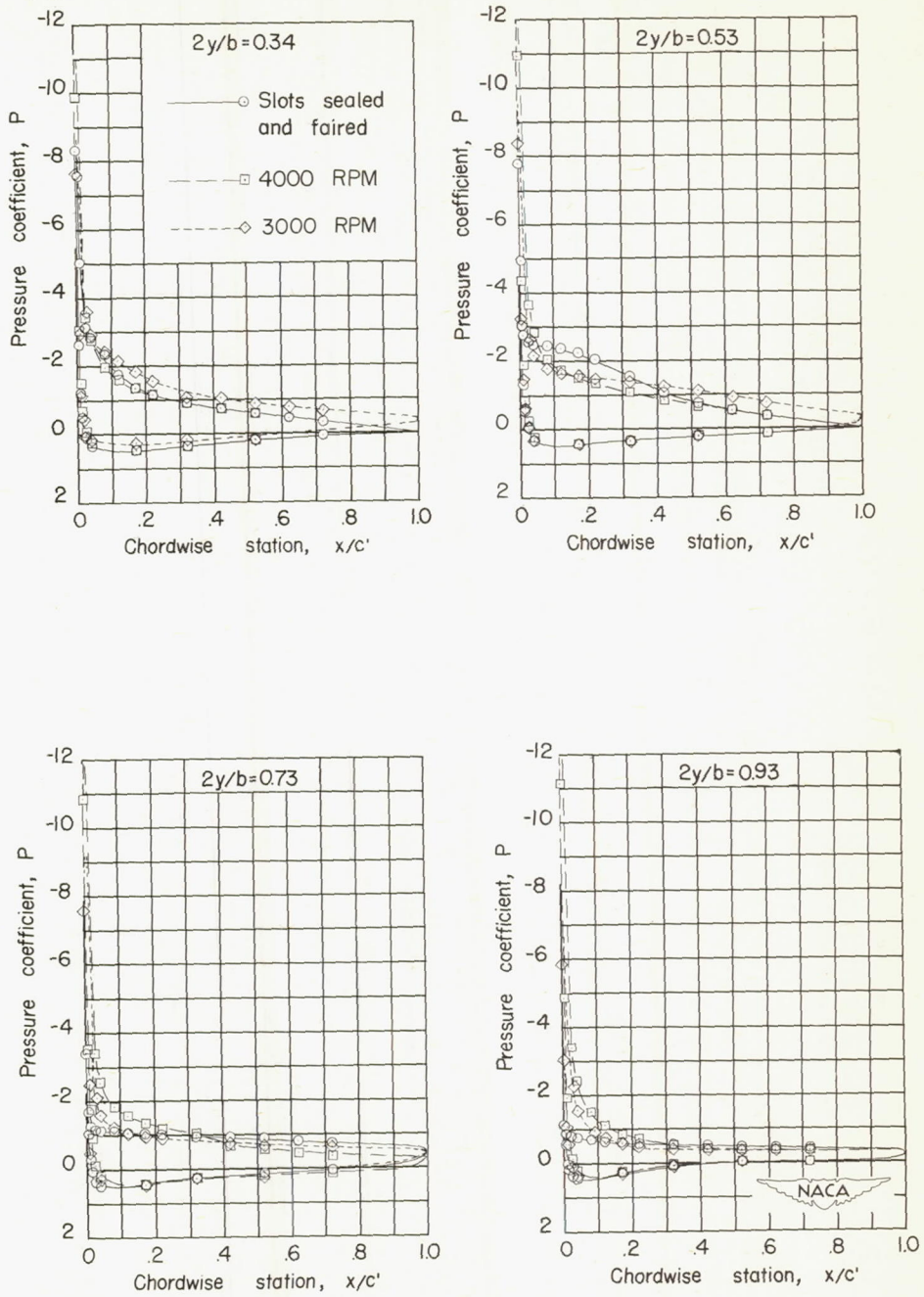

(c) $\alpha = 18.1^{\circ}$.

Figure 11.- Continued.

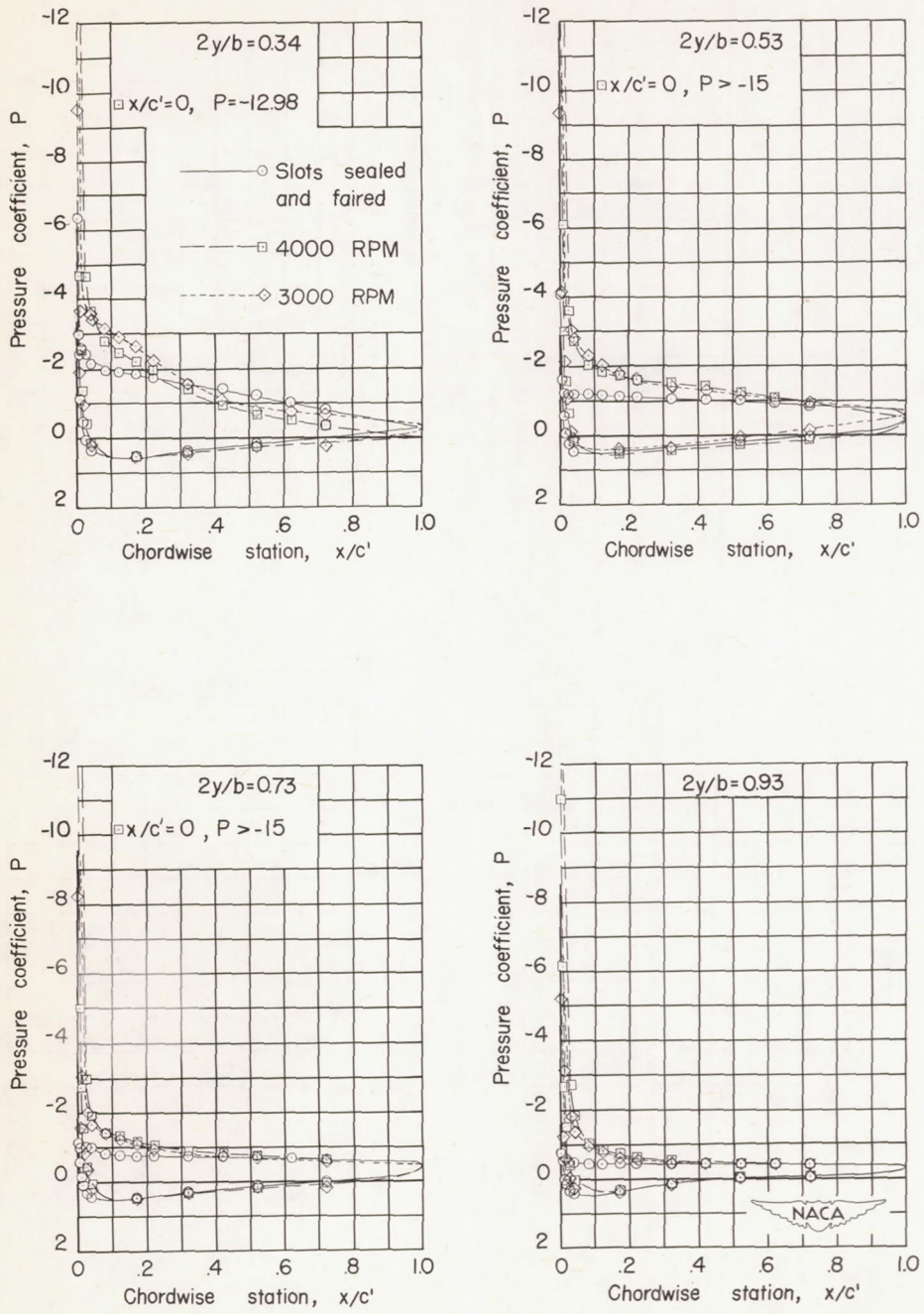

(d) $\alpha = 21.9^{\circ}$.

Figure 11.- Concluded.

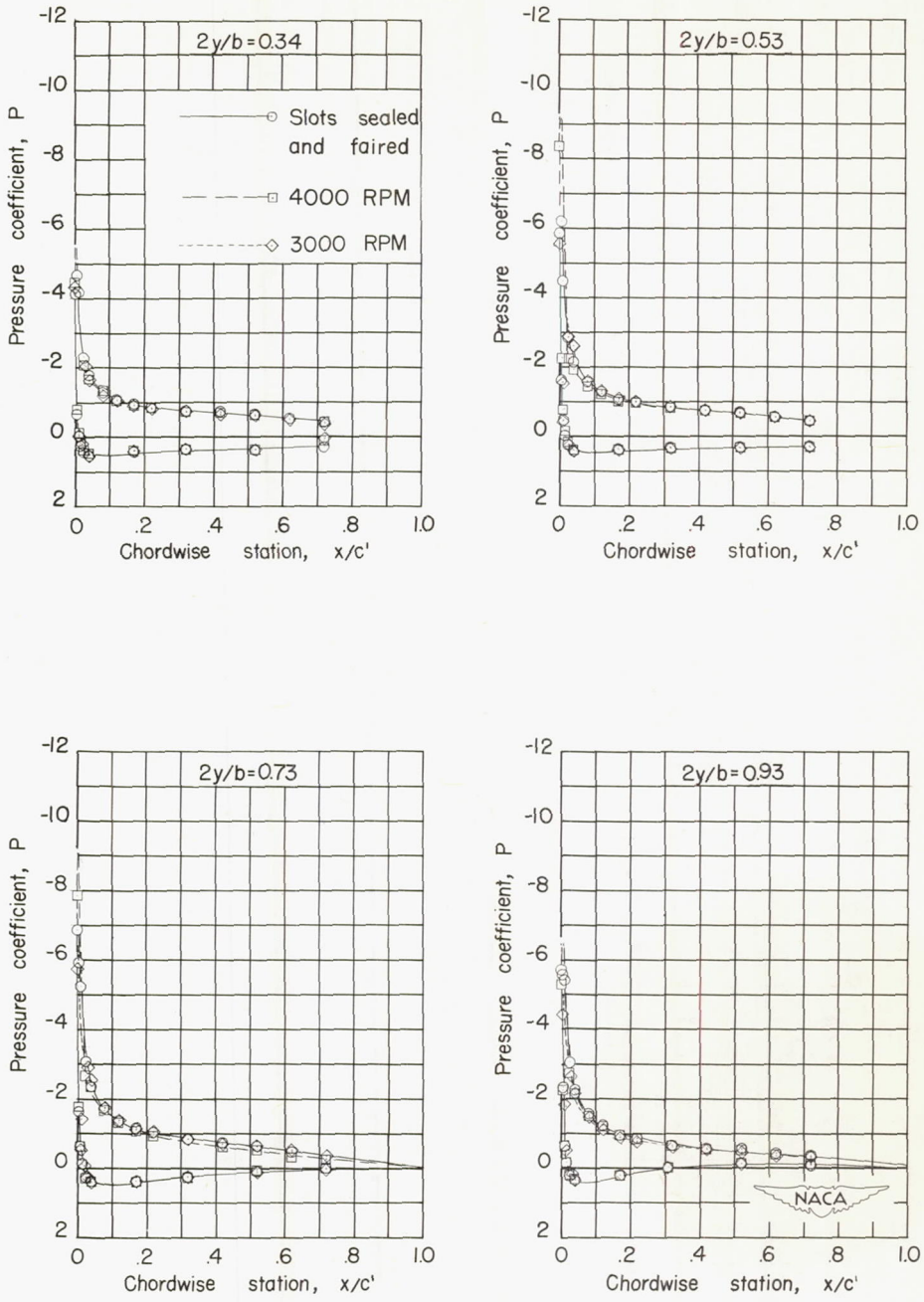

(a) $\alpha = 10.3^{\circ}$.

Figure 12.- Airfoil pressure distribution over a 47.5° sweptback wing with and without boundary-layer control. Semispan split flaps. 0.005c slots $\left(0.73\frac{b}{2}\right)$. $R = 6.1 \times 10^{6}$.

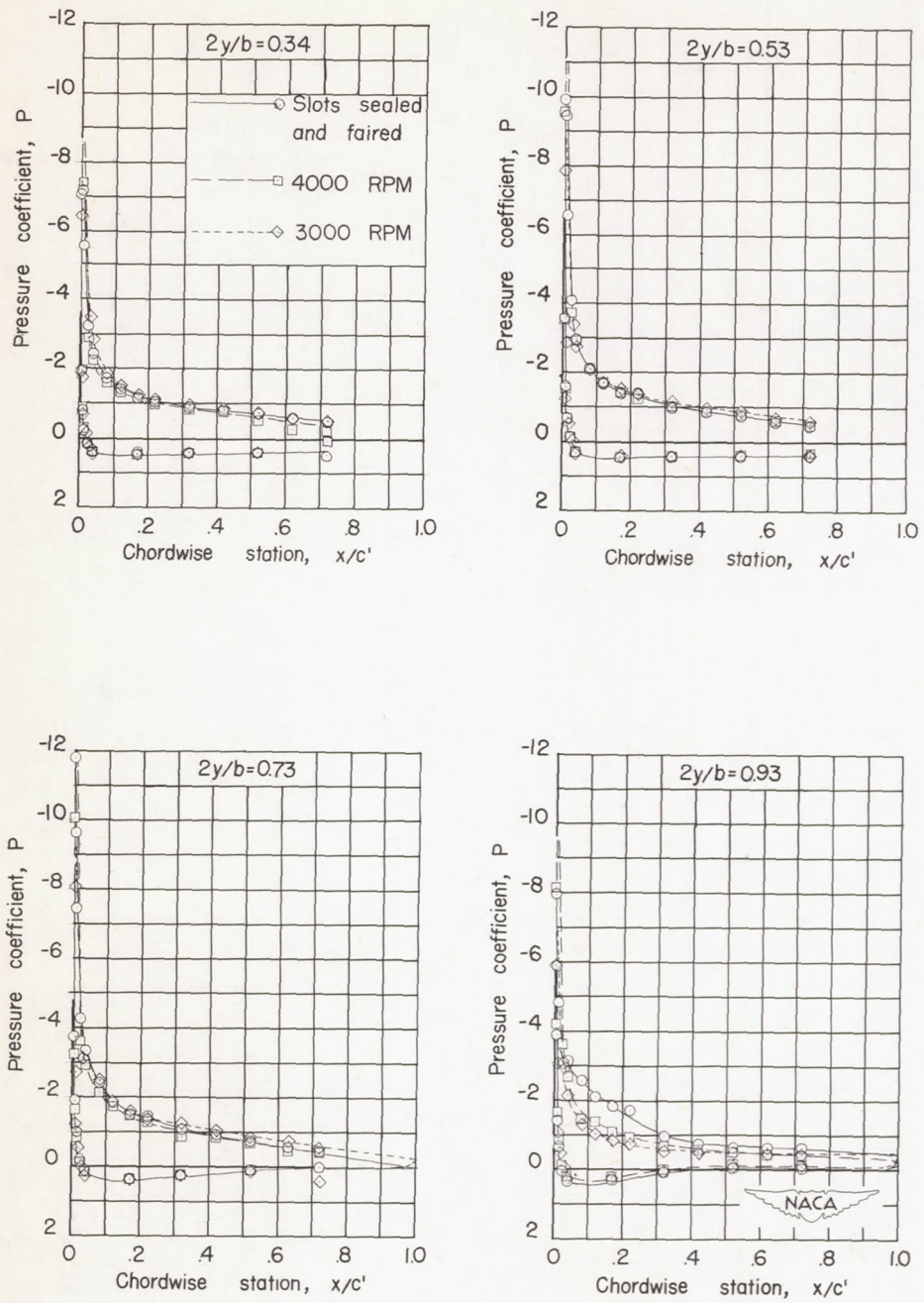

(b) $\alpha = 14^{\circ}$.

Figure 12.- Continued.

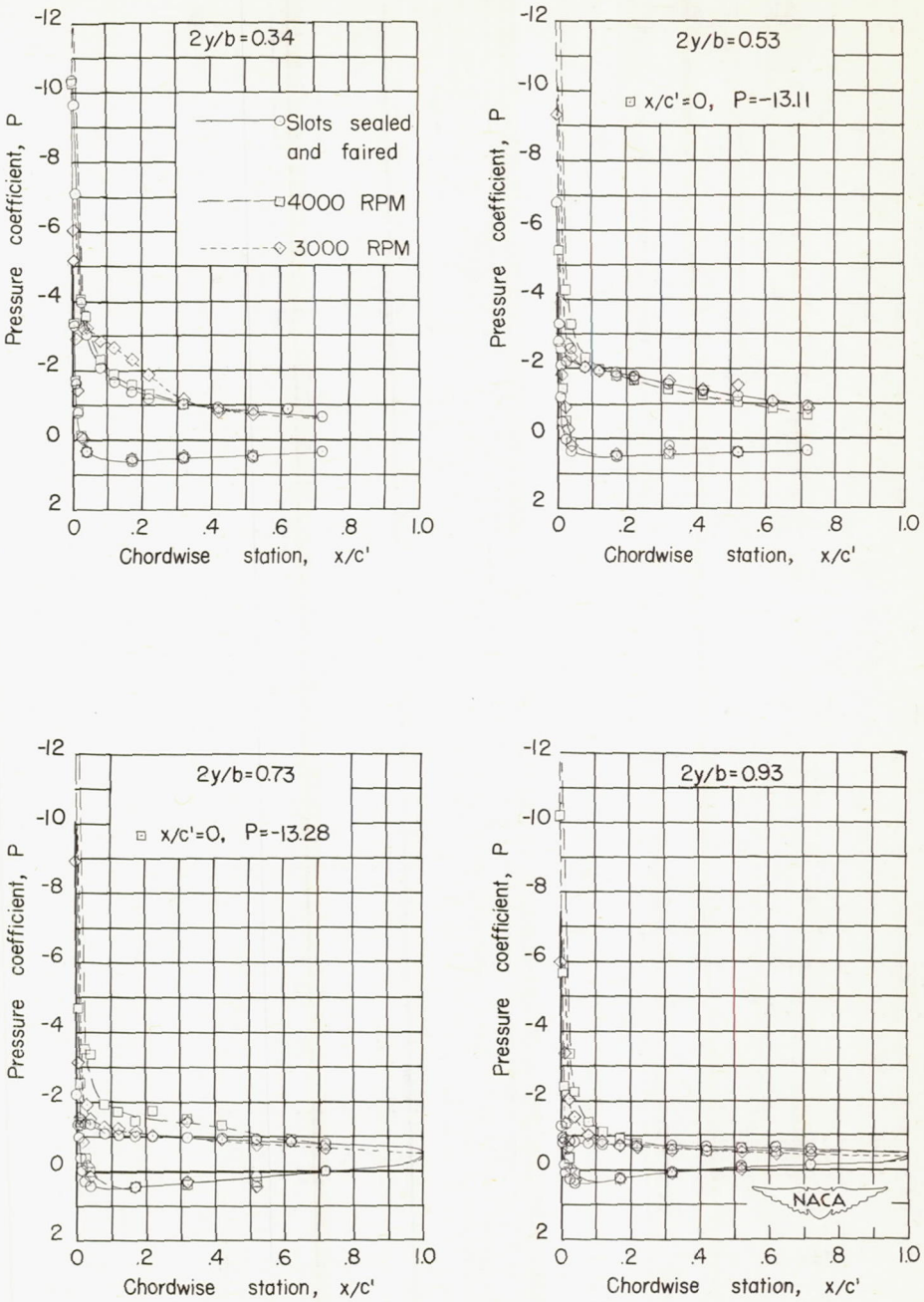

(c) $\alpha = 17.9^{\circ}$.

Figure 12.- Continued.

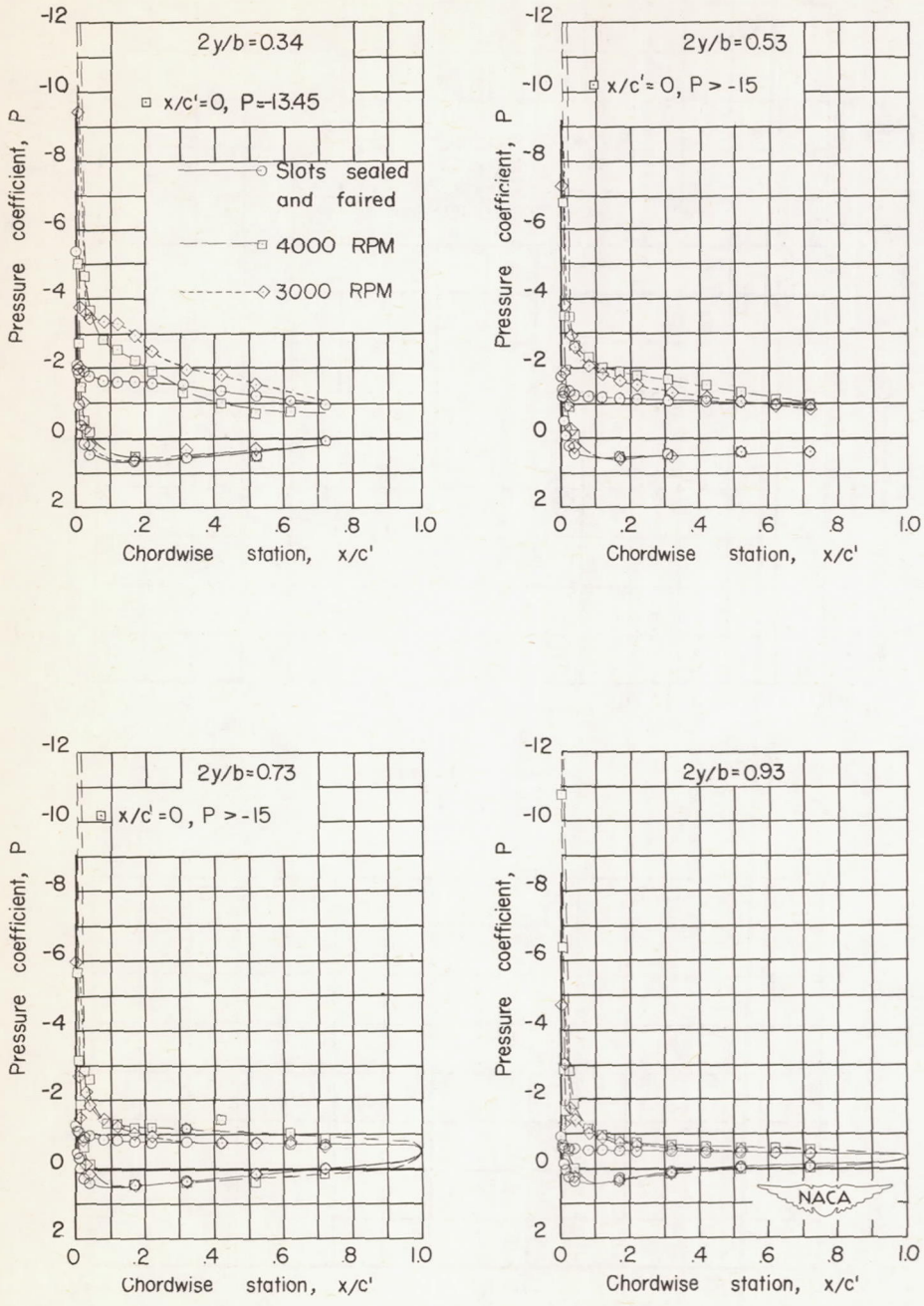

(d) $\alpha = 21.8^{\circ}$.

Figure 12.- Concluded.

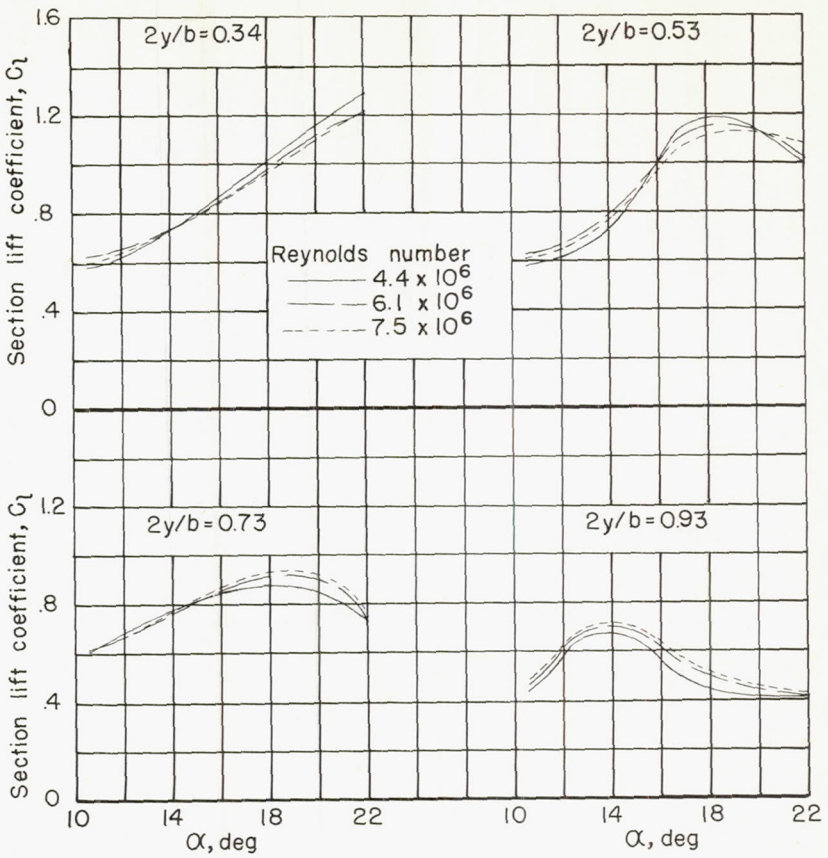

(a) Plain wing

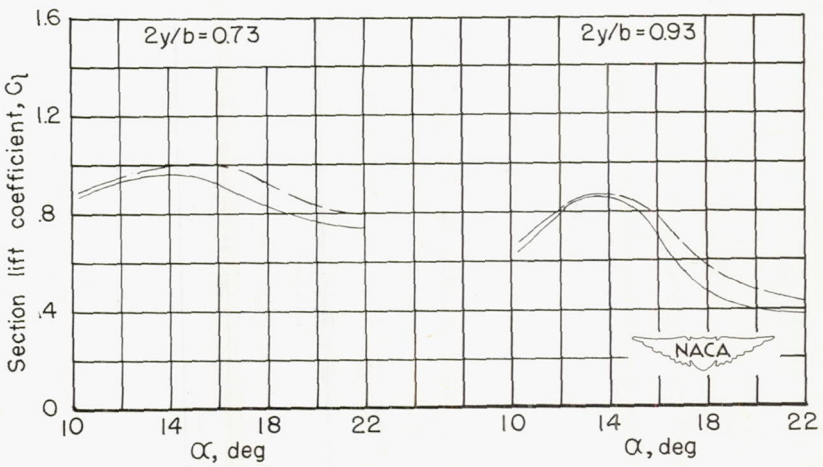

(b) Semispan split flaps.

Figure 13.- Effect of Reynolds number on the section lift characteristics of a 47.5° sweptback wing. Suction slots sealed and faired.

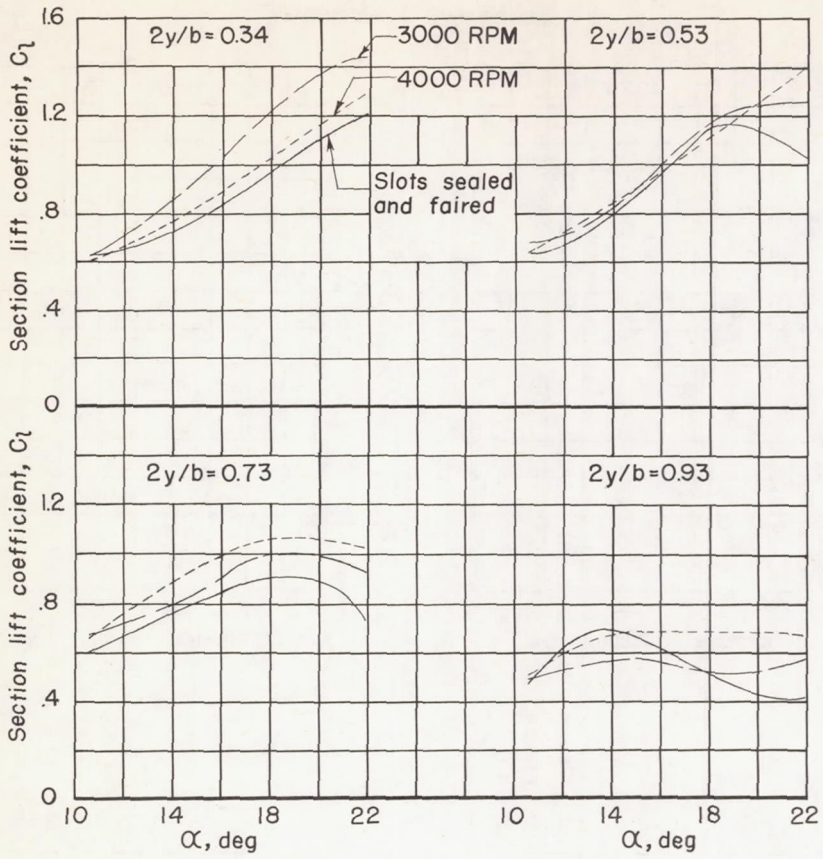

(a) Plain wing

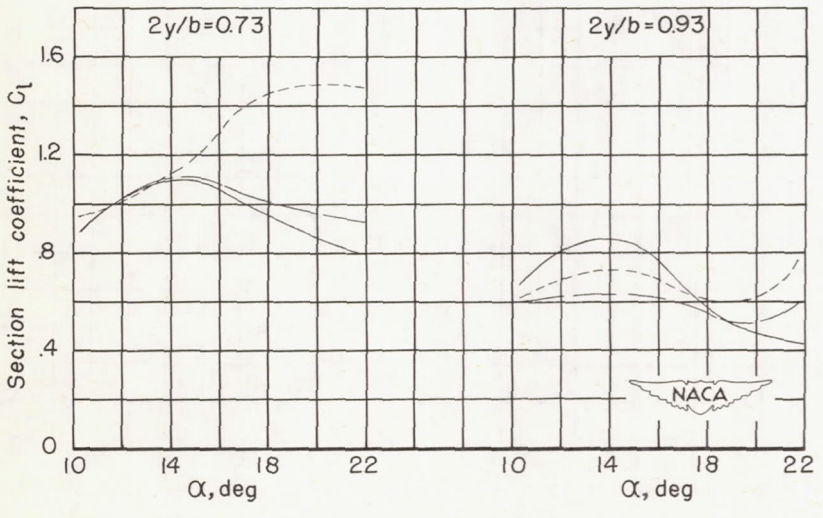

(b) Semispan split flaps.

Figure 14.- Effect of boundary-layer control by suction on the section lift characteristics of a 47.5° sweptback wing. 0.005c slots $\left(0.73\frac{b}{2}\right)$. $R = 6.1 \times 10^6$.

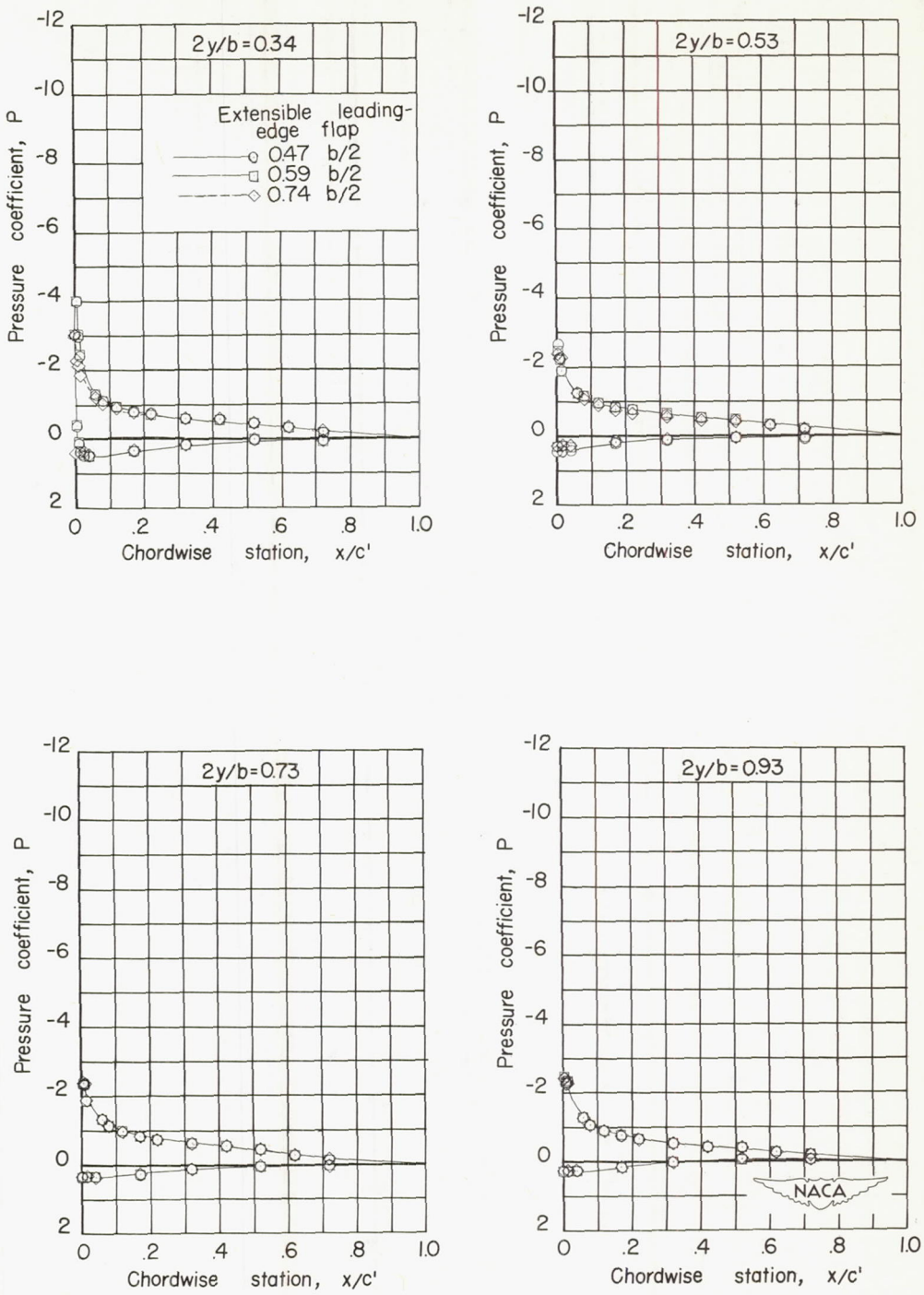

(a) $\alpha = 10.6^{\circ}$.

Figure 15.- Airfoil pressure distribution over a 47.5° sweptback wing with extensible leading-edge flaps. Slots sealed and faired. $R = 6.1 \times 10^{6}$.

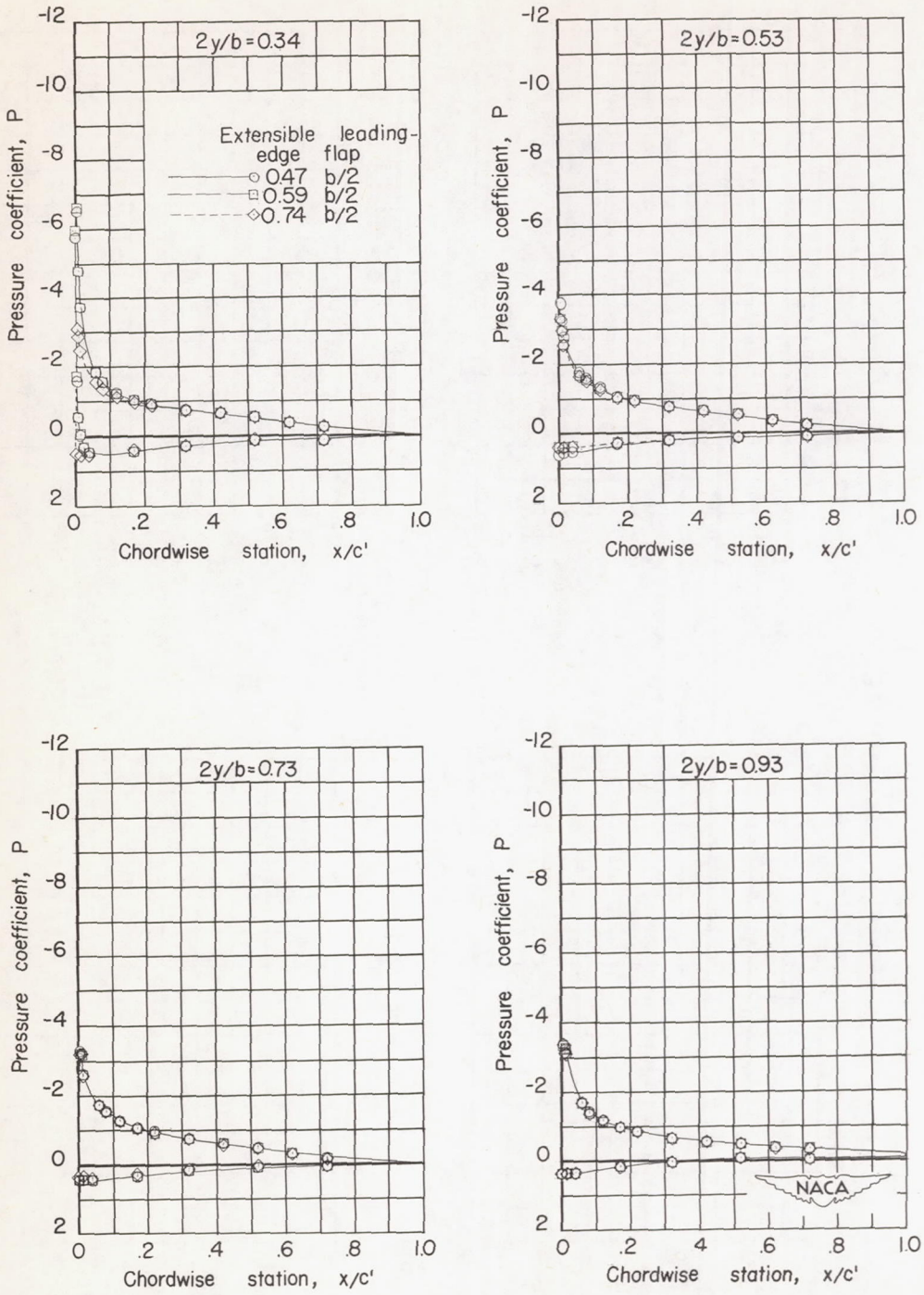

(b) $\alpha = 14.3^{\circ}$.

Figure 15.- Continued.

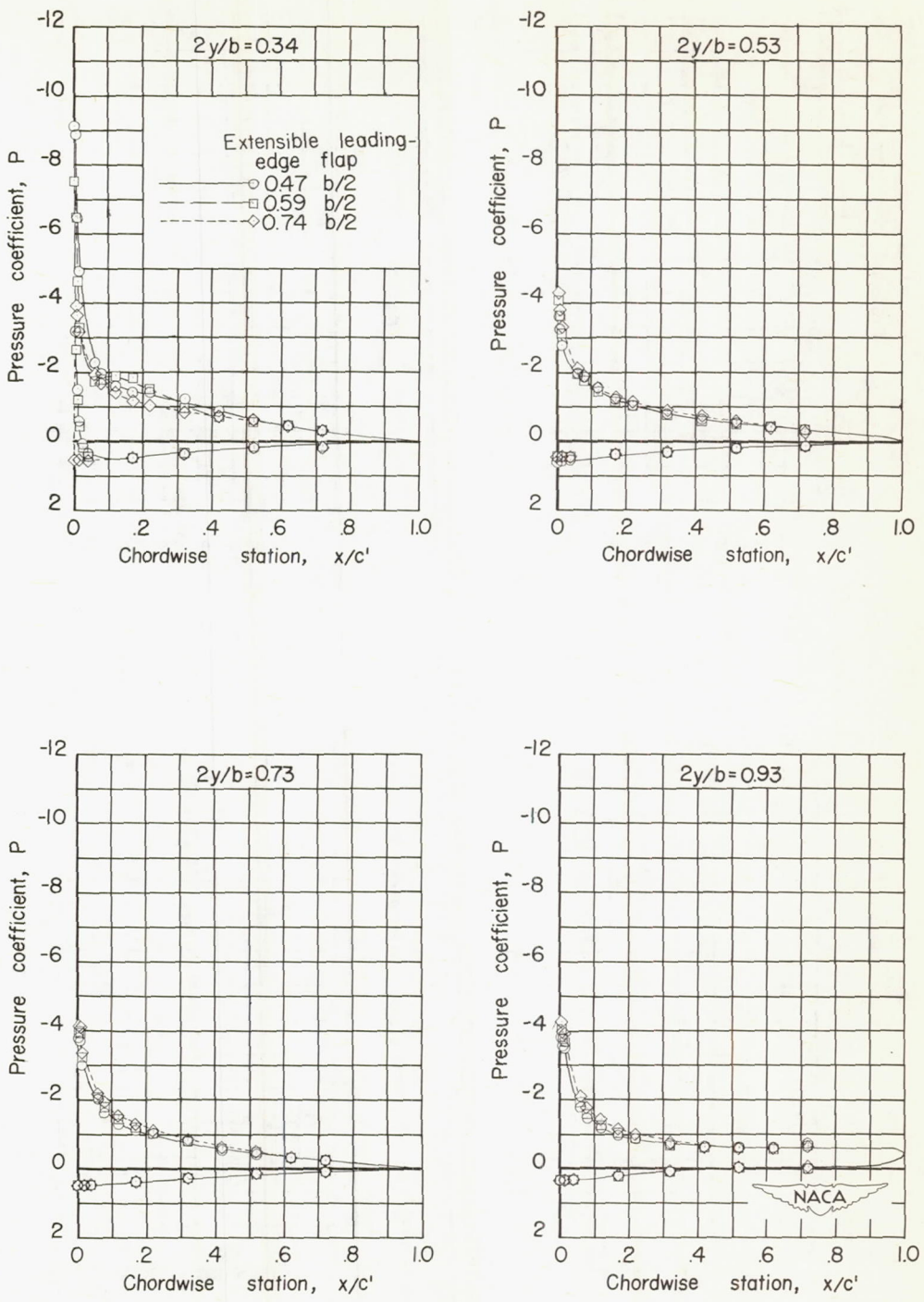

(c) $\alpha = 18^{\circ}$.

Figure 15.- Continued.

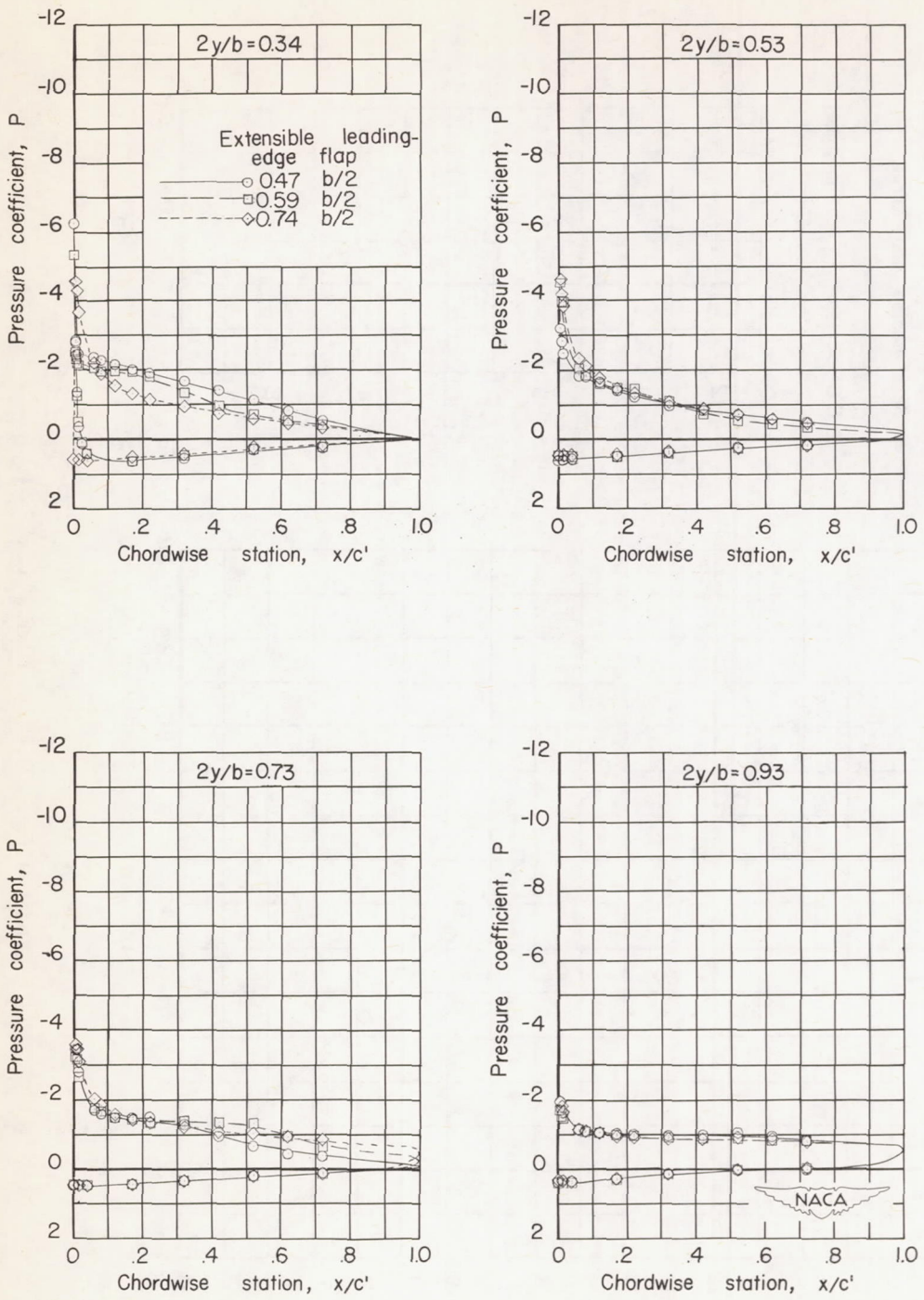

(d) $\alpha = 21.8^{\circ}$.

Figure 15.- Concluded.

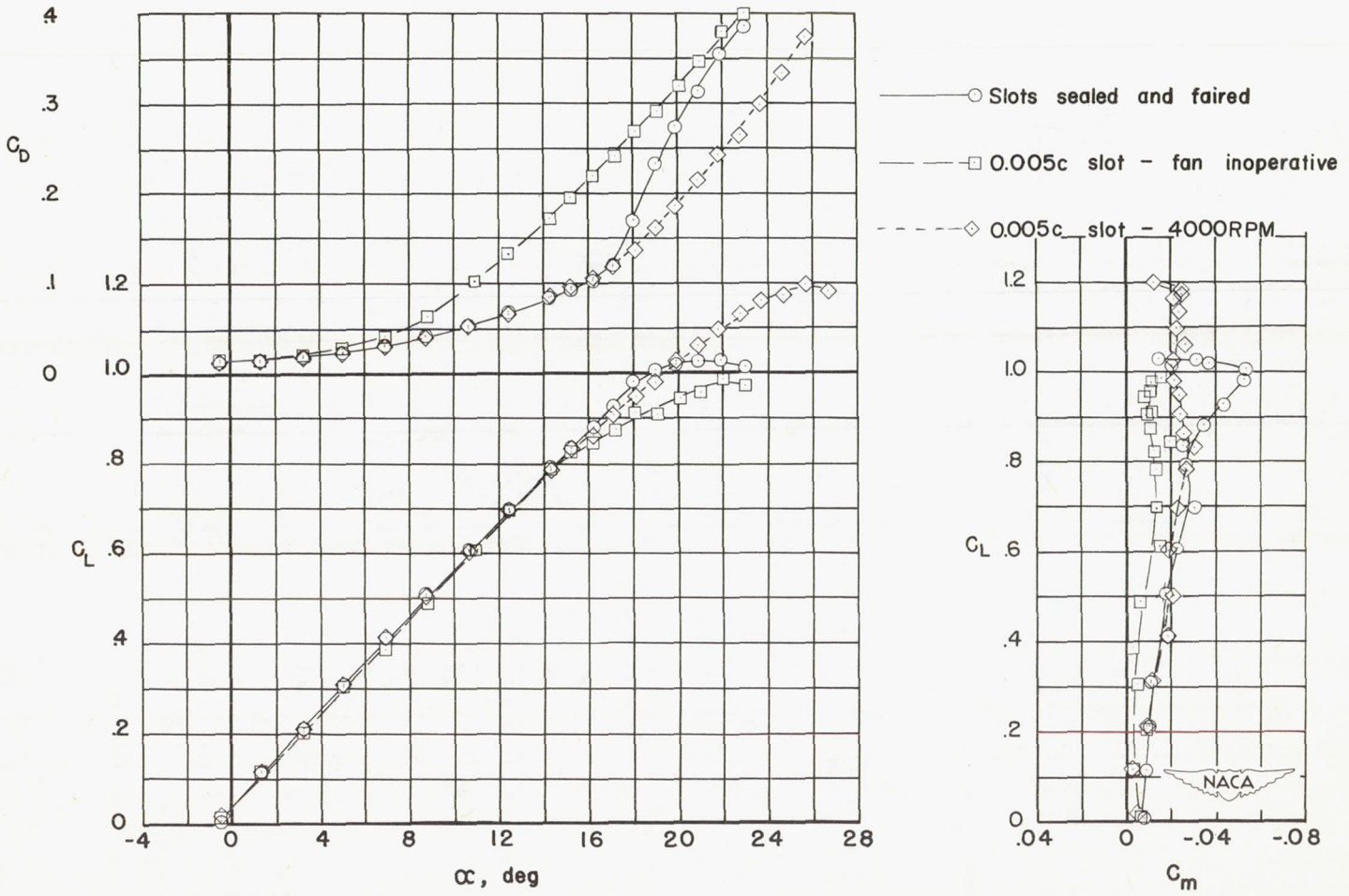

(a) Plain wing. 0.005c slots $\left(0.73\frac{b}{2}\right)$.

Figure 16.- Effect of suction-power failure on the aerodynamic characteristics of a 47.5° sweptback wing-fuselage combination. R = 6.1 × 10^6.

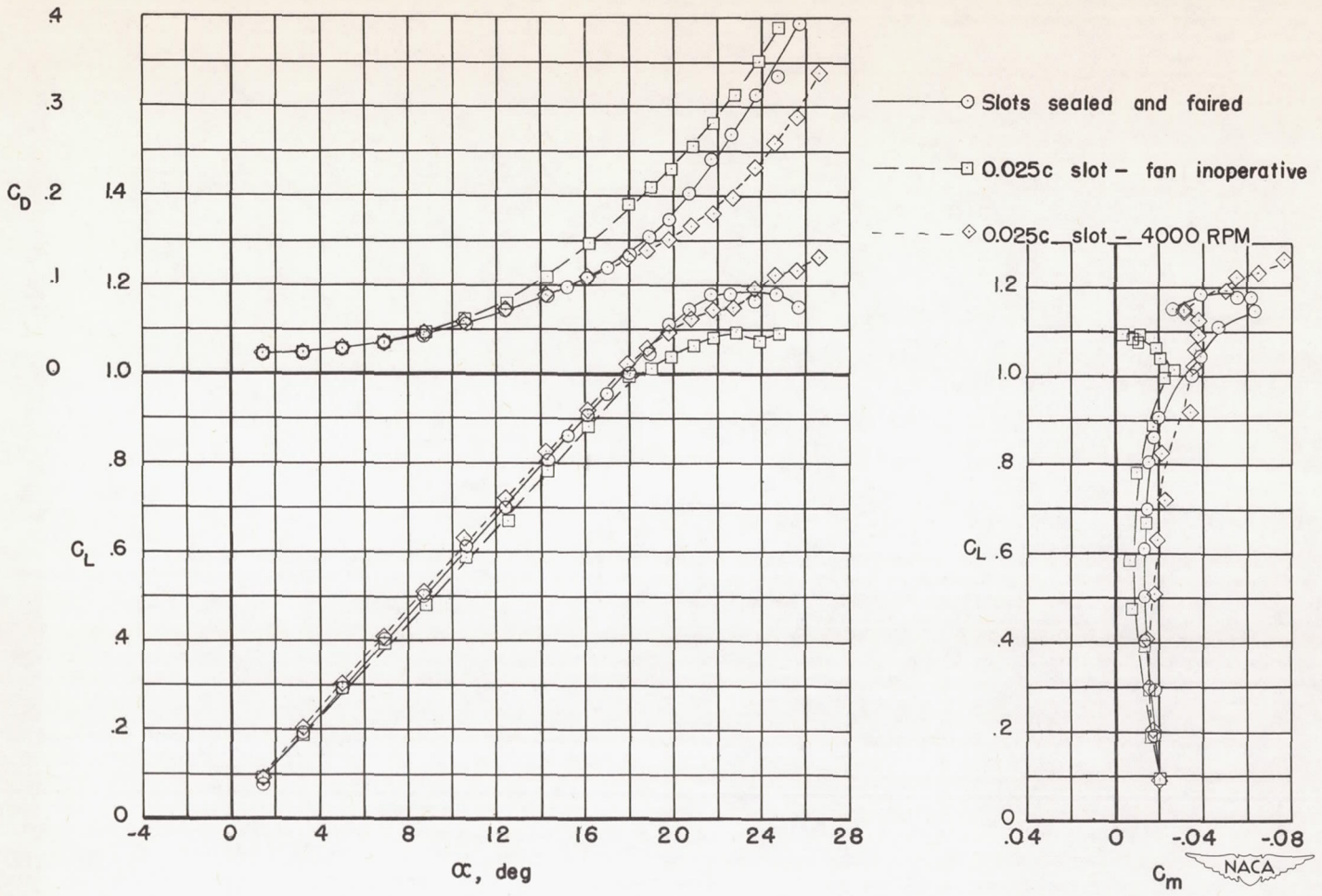

(b) $0.74\frac{b}{2}$ extensible leading-edge flaps. 0.025c slots $\left(0.73\frac{b}{2}\right)$.

Figure 16.- Concluded.